(2)

NAVAL POSTGRADUATE SCHOOL

Monterey, California

THESIS

FLIGHT TESTING OF A HALF-SCALE
REMOTELY PILOTED VEHICLE

by

Paul A. Koch

March 1992

Thesis Advisor: Richard M. Howard

Unclassified
SECURITY CLASSIFICATION OF THIS PAGE

REPORT DOCUMENTATION PAGE

1a REPORT SECURITY CLASSIFICATION Unclassified	1b RESTRICTIVE MARKINGS
2a SECURITY CLASSIFICATION AUTHORITY	3 DISTRIBUTION/AVAILABILITY OF REPORT Approved for public release; distribution is unlimited
2b DECLASSIFICATION/DOWNGRADING SCHEDULE	
4 PERFORMING ORGANIZATION REPORT NUMBER(S)	5 MONITORING ORGANIZATION REPORT NUMBER(S)
6a NAME OF PERFORMING ORGANIZATION Naval Postgraduate School 6b OFFICE SYMBOL (*If applicable*) AA	7a. NAME OF MONITORING ORGANIZATION Naval Postgraduate School
6c ADDRESS (*City, State, and ZIP Code*) Monterey, CA 93943-5000	7b ADDRESS (*City, State, and ZIP Code*) Monterey, CA 93943-5000
8a. NAME OF FUNDING/SPONSORING ORGANIZATION 8b OFFICE SYMBOL (*If applicable*)	9. PROCUREMENT INSTRUMENT IDENTIFICATION NUMBER
8c ADDRESS (*City, State, and ZIP Code*)	10. SOURCE OF FUNDING NUMBERS Program Element No. / Project No. / Task No. / Work Unit Accession Number

11 TITLE (*Include Security Classification*)
Flight Testing of a Half-Scale Remotely Piloted Vehicle

12 PERSONAL AUTHOR(S) Koch, Paul A.

13a TYPE OF REPORT	13b TIME COVERED	14 DATE OF REPORT (*year, month, day*)	15. PAGE COUNT
Master's Thesis	From To	1992 March	82

16 SUPPLEMENTARY NOTATION
The views expressed in this thesis are those of the author and do not reflect the official policy or position of the Department of Defense or the U.S. Government.

17. COSATI CODES			18. SUBJECT TERMS (*continue on reverse if necessary and identify by block number*)
FIELD	GROUP	SUBGROUP	RPV, Telemetery, Longitudinal Stability

19 ABSTRACT (*continue on reverse if necessary and identify by block number*)

Flight testing of a half-scale Pioneer remotely piloted vehicle was conducted to determine the longitudinal static stability flying qualities. A pulsewidth modulated telemetery system was used to provide data on control surface deflections, angle of attack, sideslip angle and airspeed. From the testing, the neutral point of was determined to be 41.2% of mean aerodynamic chord, which was within 13% of theoretical predictions. On a subsequent flight, the Pioneer experienced electromagnetic interference which caused the disruption of the flight control uplink signal, causing it to fly uncontrolled into the ground. Simultaneous playback of video and time histories of downlink data was instructional in analyzing the interference leading to the accident

20. DISTRIBUTION/AVAILABILITY OF ABSTRACT	21. ABSTRACT SECURITY CLASSIFICATION	
☒ UNCLASSIFIED/UNLIMITED ☐ SAME AS RPT. ☐ DTIC USERS	Unclassified	
22a NAME OF RESPONSIBLE INDIVIDUAL Richard M. Howard	22b TELEPHONE (*Include Area code*) (408) 646-2870	22c OFFICE SYMBOL AA Ho

DD FORM 1473, 84 MAR — 83 APR edition may be used until exhausted. All other editions are obsolete.

SECURITY CLASSIFICATION OF THIS PAGE
Unclassified

Approved for public release; distribution is unlimited.

FLIGHT TESTING OF A HALF-SCALE REMOTELY PILOTED VEHICLE

by

Paul A. Koch
Lieutenant, United States Navy
B.A., Miami University, 1985
B.S., Miami University, 1985

Submitted in partial fulfillment
of the requirements for the degree of

MASTER OF SCIENCE IN AERONAUTICAL ENGINEERING

from the

NAVAL POSTGRADUATE SCHOOL
March 1992

Author: 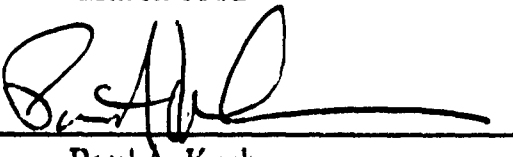
Paul A. Koch

Approved by: 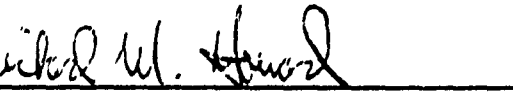
Richard M. Howard, Thesis Advisor


Louis V. Schmidt, Second Reader


Daniel J. Collins, Chairman
Department of Aeronautics and Astronautics

ABSTRACT

Flight testing of a half-scale Pioneer remotely piloted vehicle was conducted to determine the longitudinal static stability flying qualities. A pulsewidth modulated telemetry system was used to provide data on control surface deflections, angle of attack, sideslip angle and airspeed. From the testing, the neutral point was determined to be 41.2% of mean aerodynamic chord, which was within 13% of theoretical predictions. On a subsequent flight, the Pioneer experienced electromagnetic interference which caused the disruption of the flight control uplink signal, causing it to fly uncontrolled into the ground. Simultaneous playback of video and time histories of downlink data was instructional in analyzing the interference leading to the accident.

TABLE OF CONTENTS

LIST OF SYMBOLS

α	Angle of attack
ß	Sideslip angle
δ_a	Aileron deflection, + right aileron up
δ_e	Elevator deflection, + trailing-edge up
δ_r	Rudder deflection, + trailing-edge right
C_L	Lift coefficient
$C_{L\alpha}$	Lift coefficient change with change in α
$C_{L\delta e}$	Lift coefficient change with elevator deflection
C_M	Pitching moment coefficient
$C_{M\alpha}$	Pitching moment coefficient with change in α
$C_{M_{cg}}$	Pitching moment coefficient about center-of-gravity
CG	Center of gravity
DC	Direct current
EMI	Electromagnetic interference
h_n	Neutral point, percent of MAC
h	Center-of-gravity location, percent of MAC
Hz	Hertz
KIAS	Knots, indicated airspeed
lbs	Pounds
MAC	Mean aerodynamic chord
mAh	Milliamperes per hour
MHz	Megahertz
MPH	Miles-per-hour
ms	Microseconds
mW	Milliwatt
NiCad	Nickel Cadmium
UHF	Ultra high frequency
$\overline{V}$	Tail volume ratio
Vdc	Volts, dc
V_{max}	Maximum airspeed

ACKNOWLEDGMENTS

There were many people involved in this project to whom I owe my deepest appreciation. A very special thanks to Mr. Don Meeks. His wealth of knowledge and airmanship with radio-controlled models is truly amazing. A special thanks also to Lt. Paul Merz, who graciously volunteered his personal time to teach me the art of radio-controlled model repair. I am also grateful to Dr. Richard Howard for all his patience, understanding and words of encouragement throughout the entire project. It was indeed a pleasure to work for him.

Finally, to the two individuals who perhaps sacrificed the most, my wife Katherine and son Andrew, I give an extra-special thank you. Their patience and selflessness over the course of my work here has been admirable. I could not have done it without them.

I. INTRODUCTION

Radio-control modelers for years have flown scaled aircraft for recreation, unaware of the potential engineering tool that lay at their finger-tips. In recent years, scaled modeling has found a home in flight test in such areas as high angle-of-attack and post-stall flight. Past work by the National Aeronautics and Space Administration (NASA) include 1/4-scale model testing of a spin-resistant trainer to determine stall and spin characteristics [Ref. 1], modified configuration flight testing of the Exdrone remotely piloted vehicle (RPV) [Ref. 2], and lateral stability analysis of a 22% dynamically scaled X-29A model [Ref. 3]. In fact, Raney and Batterson [Ref. 3] claim that "tests of dynamically scaled model airplanes continue to be the most reliable source of information on high angle of attack, flight dynamic characteristics prior to the actual flight test of a particular aircraft." Using unmanned air vehicles (UAVs), an engineer can test radical design concepts and obtain qualitative as well as quantitative information on an aircraft without risking loss of expensive full-scale prototype aircraft or human life.

The Naval Postgraduate School (NPS) Unmanned Air Vehicle Flight Research Laboratory (UAV-FRL) consists of facilities for flight test, engine power tests, wind tunnel testing and

computer modeling for its various aircraft. In addition to half-scale Pioneer flight testing, work is currently underway in the area of tilting-ducted-fan technology using the Aquila and Archytas UAVs. The Archytas, a half-scale tilting-ducted-fan technology demonstrator, designed and built at NPS, is currently being used in hover stability studies to provide data which can be used in further technology development using the modified Aquila UAV airframe. The UAV-FRL also operates a 1/7-scale F/A-18 Hornet and 1/6-scale F-16 Falcon which are used for high angle-of-attack studies. In the area of rotorcraft technologies, several scaled helicopters are being prepared for for studies in higher harmonic control (HHC) for active vibration reduction. For endurance UAV studies, a NASA Mini-Sniffer high altitude UAV is on loan from NASA. In addition, the UAV-FRL operates a U.S. Marine Corps Exdrone UAV.

The Naval Postgraduate School began its involvement in UAV flight testing in 1987 with the half-scaled Pioneer UAV in an effort to support the UAV Program office at the Pacific Missile Test Center (PMTC) at Point Mugu, California, with its flight testing of the full-scale Pioneer. During the initial PIONEER testing, several deficiencies were noted, among those discrepancies in flight test rate-of-climb, time-to-climb and fuel flow data, autopilot-related pitch instabilities, lateral control problems, maneuverability at high gross weights, and tail boom structural problems [Ref. 4:p.4.4-1].

The objective of the NPS UAV program is to develop an overall flight research program for UAVs and to investigate the correlation between the flying qualities of a scaled UAV with those of its full-scale counterpart. The research in this thesis deals with characterizing the longitudinal static stability of the Pioneer by determining the neutral point through flight testing. Flight test data obtained from the NPS Pioneer testing will be used in the initial development of a software-based Pioneer flight simulator at PMTC by the Target Simulation lab, and compared to computer panel-methods predictions and wind-tunnel results.

II. BACKGROUND

A. UNMANNED AIR VEHICLES

Successful utilization of unmanned air vehicles can be dated back as early as World War I, when small air vehicles were loaded with explosives and flown into unsuspecting targets. These systems, however crude, paved the way for the future of UAVs and, by World War II, radio-controlled drones were used as aerial targets and flying bombs. U.S. Army Air Force General Hap Arnold predicted the future of UAVs in 1945 shortly after the Japanese surrender to U.S. forces:

> We have just won a war with a lot of heros flying around in planes. The next war may be fought by airplanes with no men in them at all. It certainly will be fought with planes so far superior to those we have now that there will be no basis for comparison. Take everything you've learned about aviation in war, throw it out the window, and let's go to work on tomorrow's aviation. It will be different from anything this world has ever seen [Ref 5:p. 87].

General Arnold was right. By the Vietnam War, UAVs were used for reconnaissance and intelligence gathering in areas too heavily defended by surface-to-air missile (SAM) and anti-aircraft artillery (AAA) sites for manned aircraft.

In June 1982, Israeli forces invaded Syrian forces in Lebanon's Bekaa Valley. At the battle's end, 79 Syrian aircraft and 19 Syrian SAM sites were destroyed with only one Israeli aircraft lost. Much of the Israeli success was attributed to their use of the Scout and Mastiff UAVs. By

first using UAVs to locate and classify Syrian SAM and AAA locations, the Israelis were able to use UAVs as decoys for manned aircraft equipped with anti-radiation missiles (ARM). [Ref. 5:p. 6]

Shortly following, in December 1983, the U.S. Navy launched retaliatory strikes against Syrian positions in the same Bekaa Valley. The losses were heavy, with three U.S. aircraft downed by AAA fire. [Ref. 5:p. 6].

B. PIONEER UAV

It was the Israeli use of UAVs that led the Secretary of the U.S. Navy at the time, John Lehman, to issue a memorandum directing that the United States develop a Short Range UAV program for integration into the Navy and Marine Corps. The deadline for bids was September 30, 1985 with the requirement that the technology used would be off-the-shelf. In December 1985, an initial contract was awarded to the AAI Corporation of Baltimore, Maryland for delivery of three Short Range UAVs by May 1986. [Ref. 6:p. 30]

In an effort to accelerate the Navy and Marine Corps UAV capabilities, Lehman initiated the "Quick Go - Phase One" program, which requested that the Pioneer test and evaluation be run concurrent with its operational testing by the Navy and Marine Corps. As a result, the Pioneer test and evaluation began at PMTC while at the same time undergoing operational testing by the Navy at NAS Patuxent River, Maryland, and by the Marine Corps at Marine Corps Base, Twentynine Palms,

California and Camp Lejune, North Carolina [Ref. 7:p. 6]. By 1987, the concept of a Short Range UAV as an integral part of Navy and Marine Corps operations was well proven. The Pioneer is currently deployed by both the Navy and Marine Corps in such areas as battle damage assessment (BDA), tactical reconnaissance, gun fire control, and Tomahawk cruise missile over-the-horizon targeting (OTH).

The full-scale Pioneer weighs 420 pounds, has a 17-foot wingspan, and is constructed primarily of composites. It has a maximum speed of 115 MPH and flies at a maximum altitude of 15,000 feet. It is designed to carry both infrared and low light cameras. [Ref. 8:p. 10]

In Operation Desert Storm, Pioneer flew 307 flights totalling 1,011 flight hours, flying both day and night along the war's 600-mile front. For the United States, this was the first combat test of the Pioneer UAV, whose performance was impressive. The Pioneer tasking in Operation Desert Storm included reconnaissance for Navy SEAL teams, mine hunting, gunfire support and spotting Iraqi troop movement. Of the 40 to 50 PIONEERS deployed to the Persian Gulf, only seven were lost and only two were lost to enemy fire. [Ref. 9:p. 86]

C. NAVAL POSTGRADUATE SCHOOL PIONEER PROGRAM

In August 1988, the Naval Postgraduate School acquired a half-scale Pioneer UAV and in August 1989, began testing. Initial work started by Lt. James Tanner [Ref. 10] involved determining the powerplant characteristics of the O.S. MAX-108

FSR two-stroke engine installed on the Pioneer. Tanner used wind tunnel and flight testing to determine power required curves and to calculate drag polars.

In June, 1989, Capt. Daniel Lyons [Ref. 7] concluded his work with the Pioneer, which involved a computer analysis of the Pioneer configurations, large tail and small tail. Lyons used a low order panel method (PMARC) in the aerodynamic analysis to determine the static longitudinal and directional stability coefficients, as well as to determine the neutral point and cross wind limitations. The drag analysis consisted of the construction of drag polars using build-up techniques for profile drag, and a look at methods of drag reduction.

Flying qualities flight testing began in 1990 with the work of Lt. Jim Salmons [Ref. 11]. Salmons developed and installed instrumentation to measure control surface deflections, angle of attack (α), sideslip angle (β), and airspeed. His work involved testing various center of gravity (CG) configurations to determine longitudinal static stability, and constant sideslip flights to determine directional static stability. Problems with vibration, however, degraded the data recording system, rendering much of the data unusable.

Follow-on work by Lt. Kent Aitcheson [Ref. 12] in 1991 included the installation of the CHOW-1G telemetry system, designed by Lt. Kevin Wilhelm [Ref. 13], to help alleviate the problem of Salmons. Aitcheson's work included longitudinal

and directional static stability flight testing. Unfortunately, lack of sufficient data made characterizing the longitudinal and directional stability difficult.

The goal of this follow-on work is to continue with the static stability testing of Aitcheson and to gather sufficient data to accurately determine the Pioneer's neutral point. Comparison of the longitudinal stability of the scaled vehicle to wind-tunnel and numerical predictions will demonstrate the validity of scaled flight testing for static-stability parameters.

III. SYSTEM DESCRIPTION

A. GENERAL DESCRIPTION

The half-scale Pioneer UAV (Fig. 1) used by the NPS UAV-FRL is a single-engine pusher, twin-tail aircraft. The wing uses a straight Clark-Y airfoil with no aerodynamic twist or dihedral, and a chord length of 0.91 feet. The wing has been modified to include two plain flaps. The Pioneer is 5.92 feet long and has a wingspan of 8.19 feet. With full fuel, gross weight is approximately 32 lbs. [Ref. 10:p. 6]

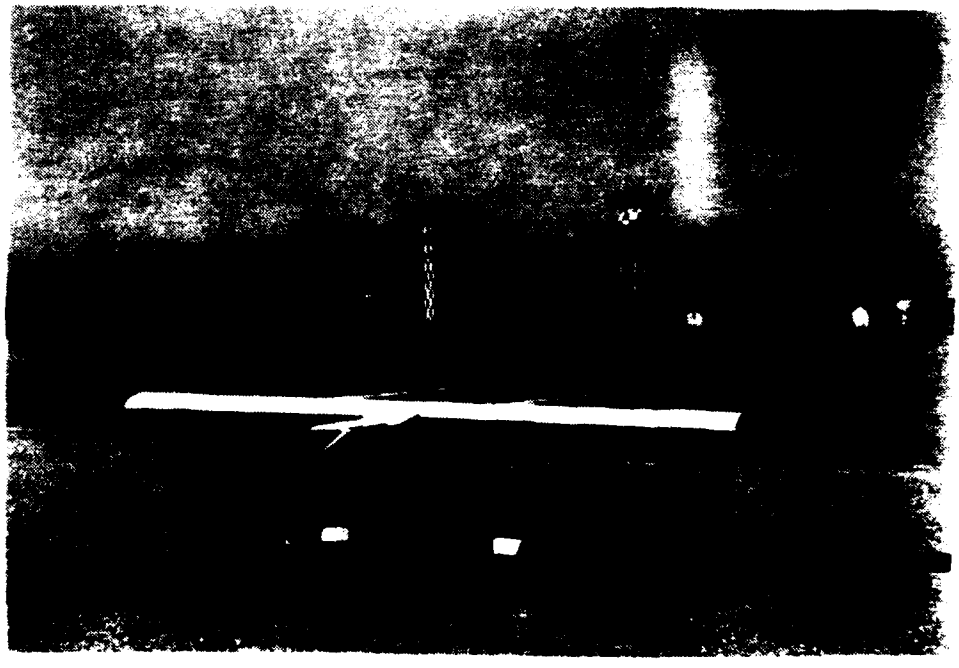

Figure 1: Half-Scale Pioneer UAV

1. Flight Control System

The Pioneer flight controls include an elevator, ailerons, twin rudders, nosewheel steering, throttle control and flaps. All flight controls are positioned using Futaba® FP-S130 high speed servos. Flight control inputs are sent by the pilot via a Futaba® FP-T9VAP pulse code modulation transmitter, transmitting at 72.710 MHz and received by a Futaba® FP-R129DP receiver. Flight control receiver inputs are sent to the control surface servos via a 21-wire ribbon bus system (Fig. 2). The entire flight control system is powered by a 4.8 Vdc, 4000 mAh NiCad battery.

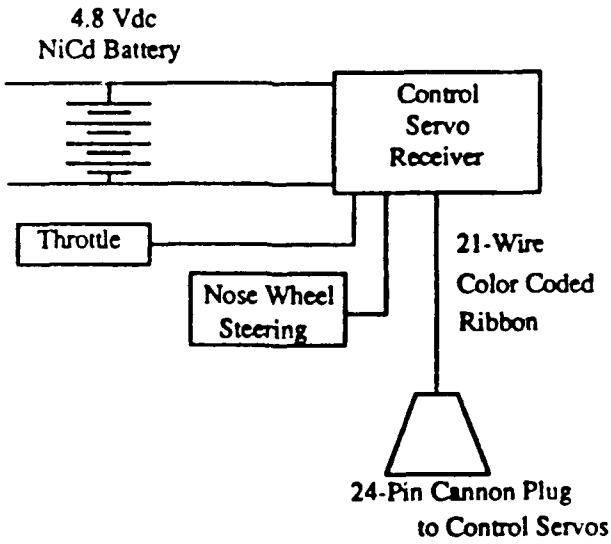

Figure 2: Flight Control System (Ref. 12)

2. Data Acquisition System

The data acquisition system encodes and transmits flight control positions, angle of attack, sideslip angle and airspeed; decodes these data on the ground; and then stores the data on magnetic tape. The system uses low-friction potentiometers to quantify control surface deflections by measuring servo movement (Fig. 3). Angle-of-attack and sideslip information is also measured using potentiometers via a probe extending in front of the Pioneer (Fig. 4). Airspeed information is sent to the telemetry system via an airspeed indicator system. The airspeed indicator system includes a pressure transducer and a signal conditioner. The output voltage is linear in a range of 40-80 KIAS. The data acquisition system is powered by a 9.6 Vdc, 500 mAh NiCad battery (Fig. 5).

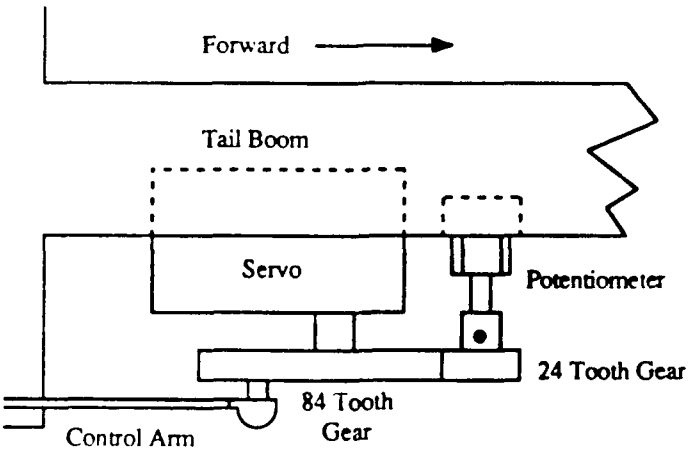

Figure 3: Rudder Potentiometer Arrangement (Ref. 12)

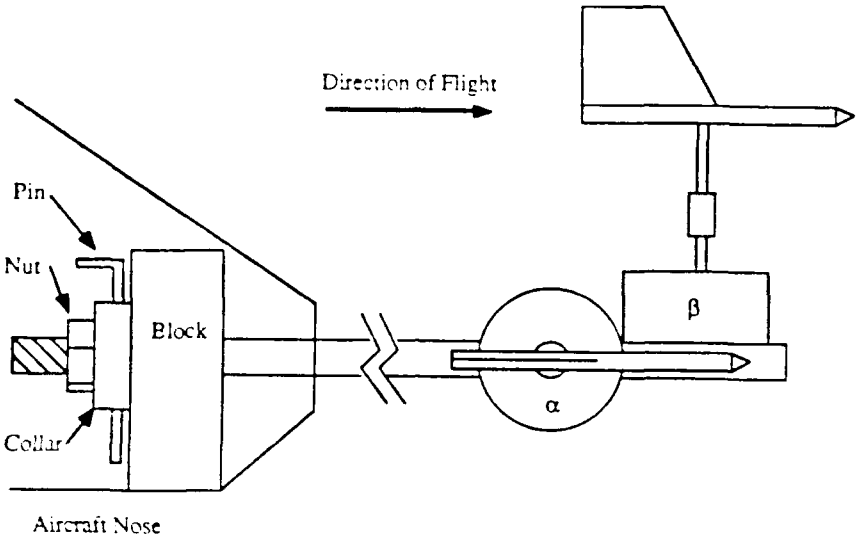

Figure 4: α-ß Probe (Ref. 12)

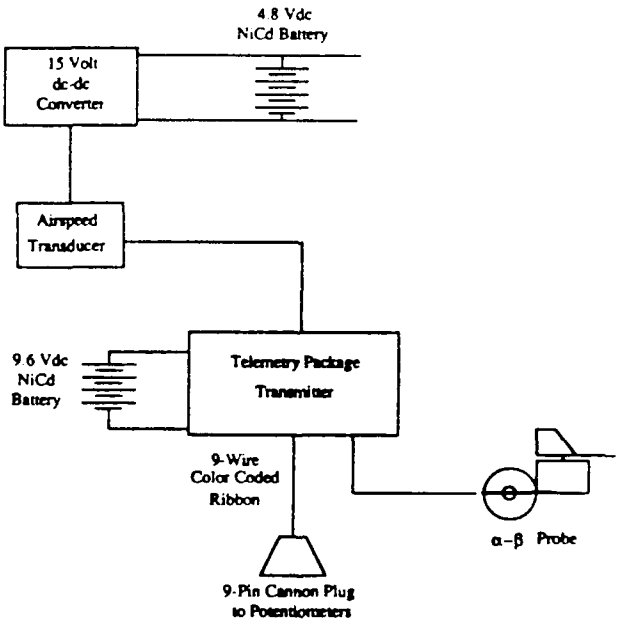

Figure 5: Data Acquisition System (Ref. 12)

B. CHOW-1G TELEMETRY SYSTEM

The CHOW-1G telemetry system was designed to help alleviate the problem of vibration effects on data acquisition. Additionally, by removing the recording unit from the Pioneer, there would be a substantial weight savings. The CHOW-1G was designed as a stand-alone system which could be adapted for use in any UAV.

The CHOW-1G is actually two separate subsystems: an airborne subsystem and a ground-based subsystem. The airborne subsystem includes an encoder unit and a transmitting unit (Fig. 6). In the airborne subsystem, DC voltages from the potentiometers are converted into a seven channel pulsewidth

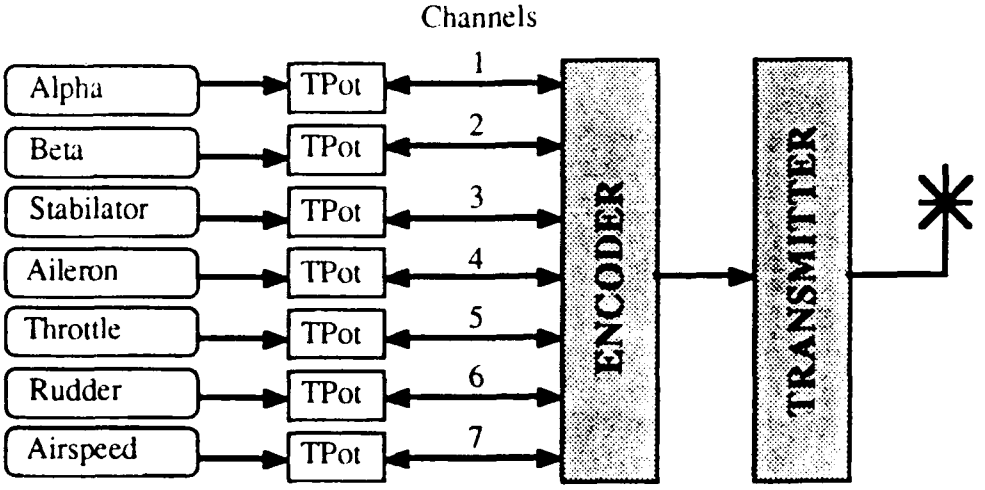

Figure 6: Airborne Subsystem (Ref. 13)

modulated (PWM) signal. This signal (Fig. 7) is a constant amplitude, variable pulsewidth signal which carries data on angle of attack, sideslip angle, stabilizer position, aileron position, rudder position, and airspeed. In the Pioneer, one channel is reserved for future use. As input voltages from each channel change, the respective pulsewidth changes. The data were sampled at 48 Hz, then sent to the transmitter and transmitted at a frequency of 27.195 MHz. [Ref. 13:p. 8]

The ground-based subsystem (Fig. 8) includes a receiver unit, a decoder unit, a recorder unit, and a display unit. In this subsystem, the transmitted signal is received, decoded from a pulsewidth to an analog voltage value, then recorded

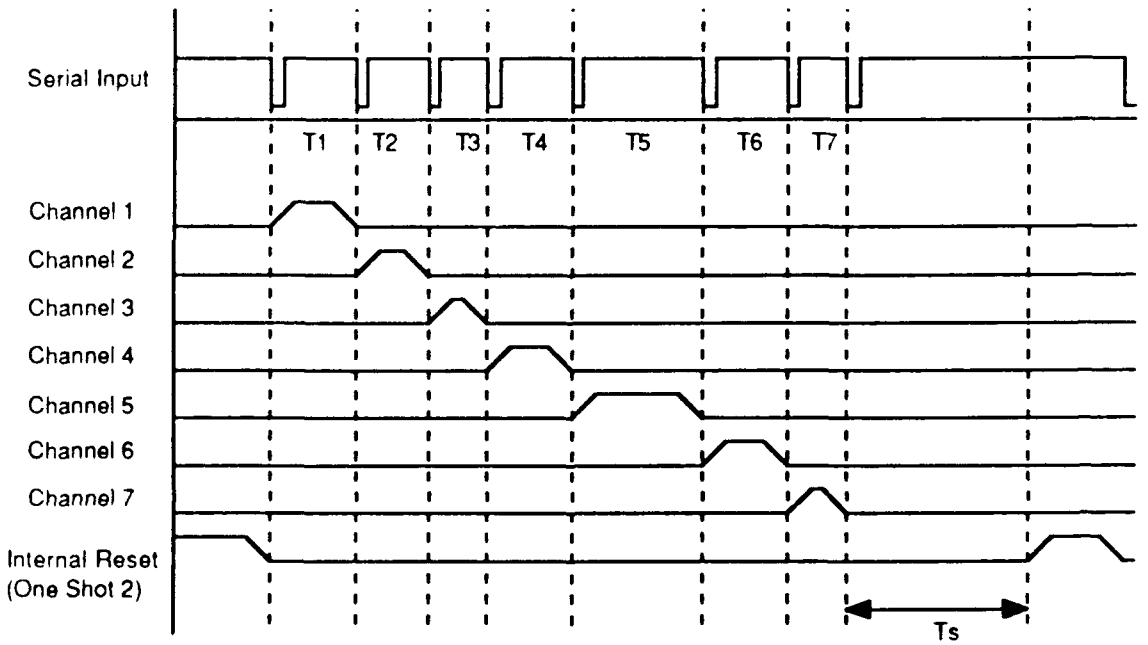

Figure 7: Signal Train Diagram (Ref. 13)

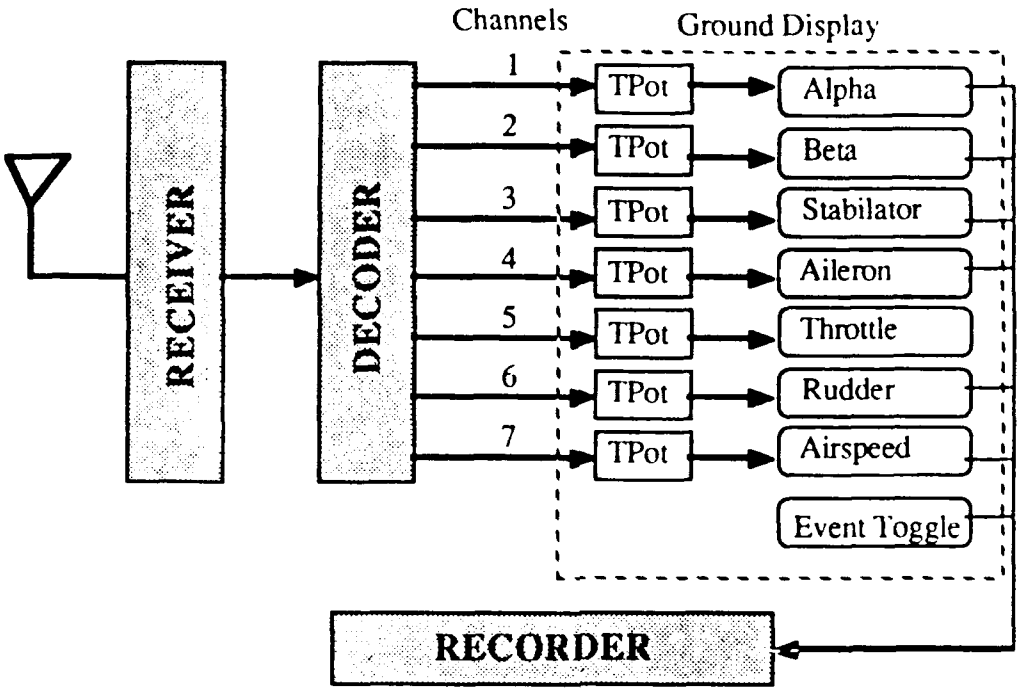

Figure 8: Ground-Based Subsystem (Ref. 13)

using a TEAC® HR-30E portable cassette data recorder. A display unit was also available to provide qualitative information on each of the channels (Fig. 9). [Ref. 13:p. 24]

C. DATA REDUCTION SYSTEM

The post-flight analysis of data was two-part. First, the continuous voltage recordings recorded on the magnetic tape by the TEAC® HR-30E cassette recorder were digitized. Second, the data were analyzed and processed using available commercial software.

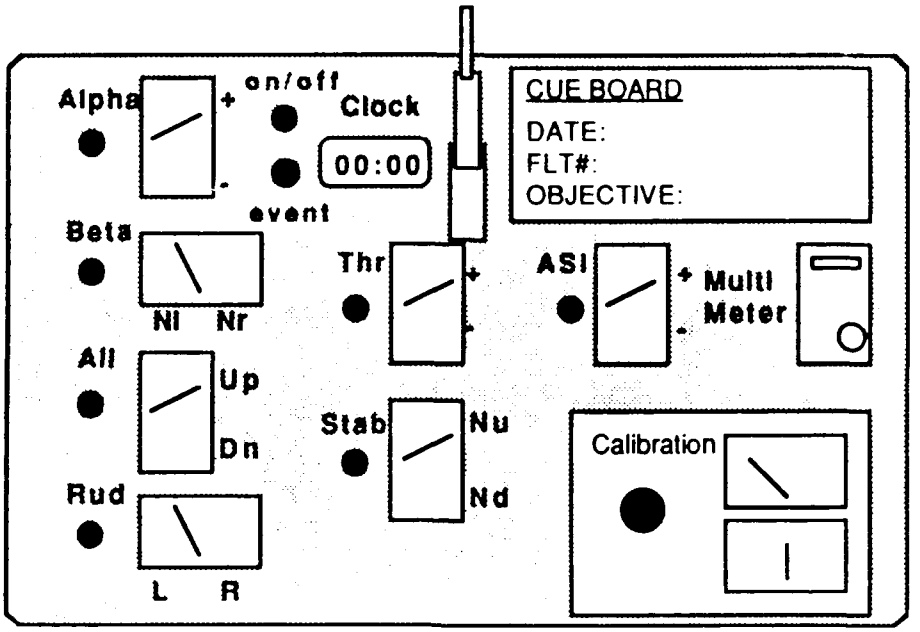

Figure 9: Ground-Based Display (Ref. 13)

1. Data Reduction

The data reduction system consisted of a TEAC® MR-30 seven-channel cassette data recorder and playback unit, an IBM personal AT computer with a Metrabyte® DASH-16F multifunction high-speed analog/digital I/O expansion board, and Labtech Notebook data acquisition and process control software. The Labtech Notebook software allowed for both normal data sampling rates (up to 150 Hz), and high speed sampling rates (20 Hz - 7000 Hz) for a seven-channel arrangement. In addition, a real-time trace of all seven data channels could be displayed in the normal mode. The data were stored as ASCII files for future analysis.

2. Data Analysis

Two software programs were used for the analysis of flight data. For the data obtained from static stability flight testing, the REDUCE program was used (Ref. 13). REDUCE is a FORTRAN program written specifically for the purpose of correlating flight test data with known calibration files. Using REDUCE, the digitized voltage values obtained during the data reduction phase are averaged, then correlated to appropriate values of control surface deflection (degrees), angle of attack and sideslip angle (degrees) and airspeed (KIAS). REDUCE assumes a linear relationship between voltages and degrees, or KIAS, and uses an average of any chosen number of data points to correlate to the calibration files. MATLAB software was used to reduce the data that were obtained using the normal sampling rates. These data were filtered using a second-order Butterworth low-pass filter to filter out much of the noise associated with the telemetry unit and carrier distortion from the playback unit [Ref. 13:p. 41]. Filtering will be discussed in detail in Chapter V.

IV. EXPERIMENTAL PROCEDURES

A. CALIBRATION

The data obtained from the flight tests were stored on magnetic tape as analog voltage values. In order for these voltages to be correlated to degrees of control deflection, degrees of sideslip or angle of attack and KIAS, they must be interpolated using known calibrated values. A detailed description of the calibration of the flight control and telemetry system is included as Appendix A. A brief description follows.

Calibration began by first adjusting the output voltages of the potentiometers by adjusting the position of the potentiometers themselves. The potentiometer output range for each channel is zero to 5 Vdc. Since there is a positive and negative value of control deflection, as well as sideslip angle and angle of attack, a neutral position voltage of 2.5 Vdc was chosen. This would allow for the measurement of movements on either side of neutral. For the airspeed transducer, a zero voltage output corresponded to 40 KIAS and a 5 Vdc voltage output corresponded to an airspeed of 80 KIAS. The airspeed values were set using the "Schmidter" pressure calibration device (see Appendix A). After each center voltage was set for each potentiometer, the pulsewidth of each individual pulse was adjusted to an optimum pulse width of 1.0

ms +/- .5 ms. With this, a .5 ms pulsewidth would correspond to an output voltage of approximately zero volts, and a 1.5 ms pulsewidth would correspond to an output voltage of 5 Vdc. These adjustments were made to all six channels by adjusting the multiplexer circuitry on the telemetry unit (see Appendix A).

With the potentiometers and telemetry unit adjusted, three calibration points were picked. Point one was with the flight controls configured with 10° up elevator, 10° up right aileron, 10° left rudder, 30° angle of attack and sideslip, and a pressure corresponding to 40 KIAS airspeed; point two was with controls neutral, angle of attack and sideslip angle neutral and airspeed 60 KIAS; and point three was with the flight controls configured with 10° down elevator, 10° up left aileron, 10° right rudder, -30° angle of attack and sideslip, and 80 KIAS airspeed. The calibration was completed prior to flight, with each point recorded through the telemetry unit and stored on magnetic tape.

Figures 8-10 show the compiled calibration curves. It must be noted that the voltages compiled through the Labtech Notebook software do not represent the true output values from the telemetry unit. While the MR-30 cassette recorder will accept input voltages up to 5 Vdc, it will only output voltage values up to 2 Vdc. As a result, all the data points obtained have been scaled down from a scale of zero to 5 Vdc to a scale of zero to 2 Vdc.

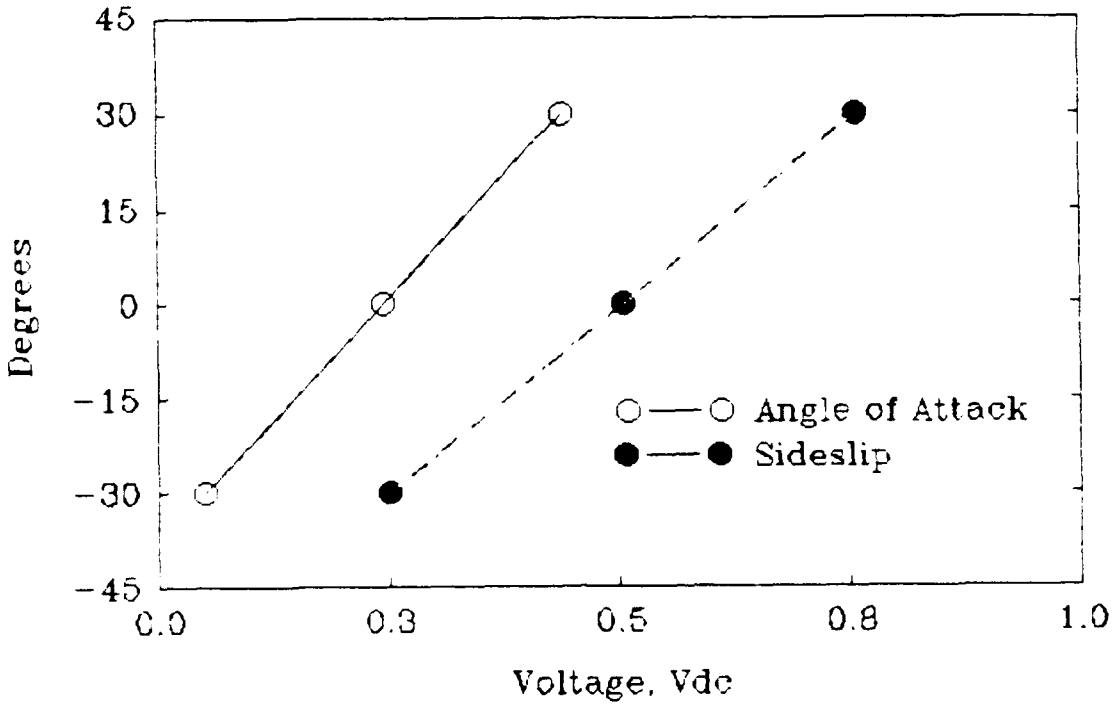

Figure 10: α-ß Calibration Curves

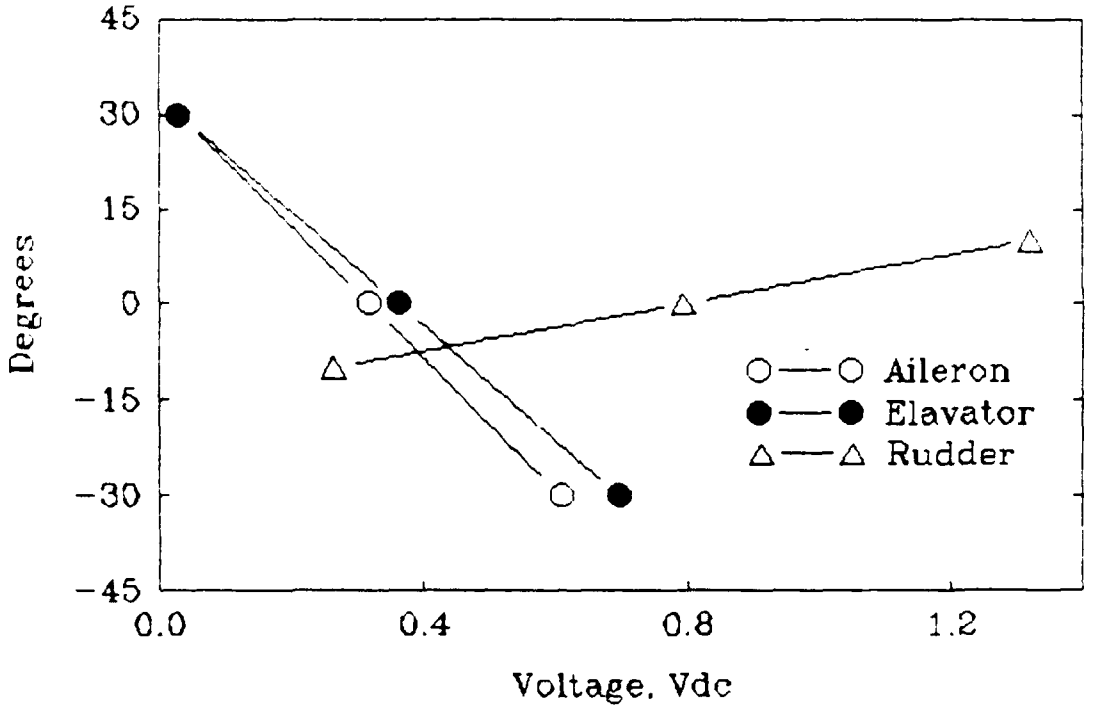

Figure 11: Control Surface Calibration Curves

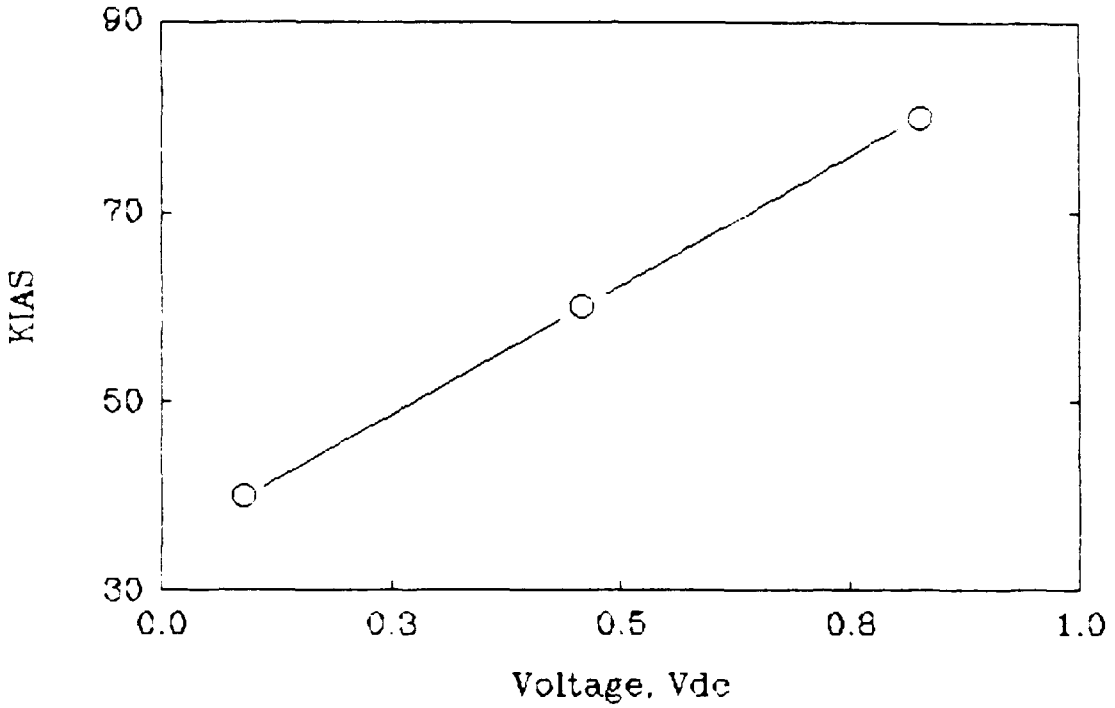

Figure 12: Airspeed Indicator Calibration Curve

B. LONGITUDINAL STATIC STABILITY

1. Theory

When discussing an aircraft's handling qualities, static stability is perhaps the most important criterion. In fact, static stability, either occurring naturally or through complex control law design, is an absolute requirement for control in flight.

An aircraft is said to be statically stable, either longitudinally in pitch, laterally in roll, or directionally in yaw, if once disturbed, forces and moments will tend to initially return the body towards its equilibrium position. Static stability deals with the initial tendency of a body to

return to equilibrium and says nothing about its behavior with time. Dynamic stability, on the other hand, deals with the time history of a body after a disturbance or perturbation. A dynamically stable aircraft will eventually return to and remain at its equilibrium position over a period of time.

When considering the three axes of rotation of an aircraft, static stability about the longitudinal axis is the most important. When defining longitudinal static stability, the pitching moment about the aircraft center-of-gravity, or $C_{M_{cg}}$, is used. More specifically, longitudinal static stability is defined in terms of the aircraft pitching moment about the center-of-gravity with respect to changes in angle of attack, or C_{M_α}. A negative value of C_{M_α} will indicate an initial tendency of the aircraft to produce a negative (nose-down) pitching moment when given a positive (nose-up) disturbance. A positive value of C_{M_α} will indicate a tendency to pitch further nose-up when responding to the same nose-up disturbance. Clearly, a statically stable aircraft will have a negative C_{M_α}.

Longitudinal static stability can be further classified as stick-fixed or stick-free. Since the flight control system on the Pioneer is irreversible, we will be dealing with stick-fixed stability only.

Another important concept in longitudinal static stability is the neutral point (h_n). Since C_{M_α} is a pitching moment coefficient change about the center of gravity, it is

easy to see that any change in the center-of-gravity location will affect the longitudinal static stability. In fact, an aircraft can be made longitudinally unstable by simple moving the center of gravity. There exists a center-of-gravity location which will allow the aircraft to become neutrally stable longitudinally. This location is called the neutral point. For an aircraft to be longitudinally stable, the center-of-gravity must be forward of the aircraft's neutral point. The distance between the center-of-gravity and the neutral point is referred to as the static margin. A positive static margin indicates static stability.

Unfortunately, it is difficult to measure pitching moments created by an aircraft that has undergone a disturbance. However, it is rather easy to determine the moment created by intentionally flying an aircraft off of a trimmed condition. In fact, if the moment created by an elevator deflection that is required to fly an aircraft at a speed other than the trimmed airspeed is known, and with the assumption that the restoring moment will be equal and opposite to the moment created by this elevator movement, C_M can be easily found using equation 4.1 [Ref. 14:p. 4.8].

$$C_{M_{aircraft}} = \overline{V} C_{L_{t_{\delta_e}}} \Delta\delta_e \qquad (4.1)$$

Differentiating with respect to coefficient of lift, C_L, gives equation 4.2 [Ref 14:p. 4.8].

$$\frac{dC_M}{dC_L} = -\overline{V} C_{L_{t_{\delta_e}}} \frac{d\delta_e}{dC_L} \qquad \textbf{(4.2)}$$

By plotting elevator deflection, δ_e, against C_L, the slope of the line, $d\delta_e/dC_L$, can be found. These plots can be compiled for various center-of-gravity positions. The slope of the lines can now be plotted against the center-of-gravity positions to yield a curve intercepting the X-axis for $d\delta_e/dC_L$ equal to zero. The restoring pitching moment is zero and that particular center-of-gravity position is the aircraft's neutral point. Once the neutral point is known, C_{M_α} can be found using equation 4.3 [Ref. 15:p.338].

$$C_{M_\alpha} = C_{L_\alpha}(h - h_n) \qquad \textbf{(4.3)}$$

2. Flight Test Procedures

All flights were flown at one of the two local flying areas at the Salinas Area Modelers airfield at Chualar, California or at Fritzsche Army Airfield located at Fort Ord, California. To provide favorable flight conditions, flights were flown in the early morning, when winds were calm.

The first series of flights took place in October 1991 at the Salinas Area Modelers field. Three flights were flown at three different center-of-gravity conditions to determine the Pioneer's neutral point. Flight one was at a center-of-gravity location of 32.34% mean aerodynamic chord (MAC), flight two was at 30.88% MAC and flight three was at 36.71% MAC. All three flights consisted of six data runs. Each run was flown at a constant altitude with successively slower airspeeds, starting with V_{max}. The airspeed on the runs varied from a maximum of 68 KIAS to a minimum of 36 KIAS. Two data points were taken for each data run, for a total of 12 data points for each center-of-gravity position. The last flight in this series ended in a hard landing which resulted in a damaged but repairable right wing.

Repairs to the Pioneer's wing were completed in November, and a familiarization (FAM) flight was flown at Fritzsche Field. As in the last series of flights, this flight was flown in the early morning. After approximately four minutes of flight time, the Pioneer experienced flight control problems which caused it to fly uncontrolled into the soft ground surrounding the runway. Unfortunately, the damage was extensive, and the Pioneer was judged unrepairable. Both mishaps will be discussed in greater detail in Chapter V.

V. RESULTS

A. LONGITUDINAL STATIC STABILITY

As mentioned earlier, the first series of flights flown in October 1991 was dedicated to longitudinal static stability and neutral-point flight testing. Three flights were flown at three different center-of-gravity locations, with the data stored on telemetry tapes. From the tapes, the data were sampled at 5000 Hz for 0.25 seconds using Labtech Notebook, yielding 1250 voltage values for each point. These values were averaged and correlated to the calibration file using the REDUCE program. A total of 12 data points were obtained for each flight. The calibrated data for each of the three center-of-gravity locations are compiled in Appendix B. The data from the last flight were found to be unusable, as airspeed information was unreliable. Angle of attack and sideslip angle data were also unusable, due to an unknown problem with the α-ß probe. However, the lack of angle of attack and sideslip angle data did not affect the calculations for determining the Pioneer's neutral point.

From the data a coefficient of lift, C_L, for each data point was calculated, then plotted against the elevator deflection, δ_e. Figures 13 and 14 show these plots for the 30.9% MAC and 32.3% MAC center-of-gravity positions. A first-order least-squares regression was used to fit the data. The

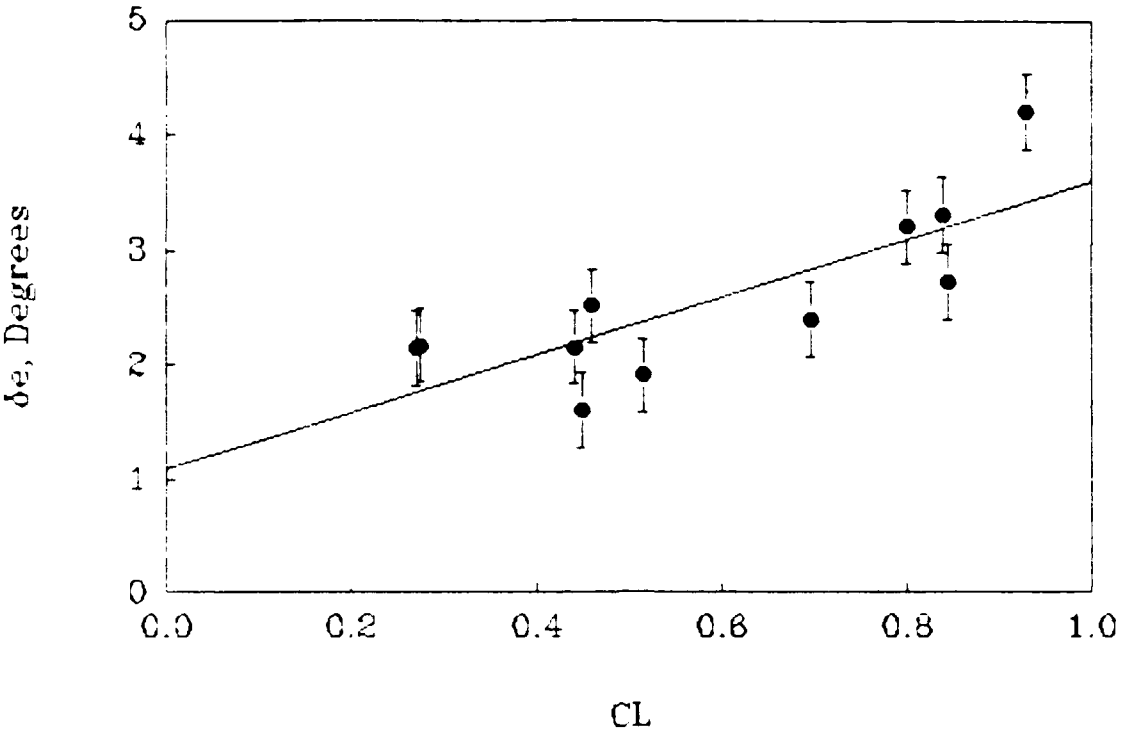

Figure 13: CG 30.9% MAC

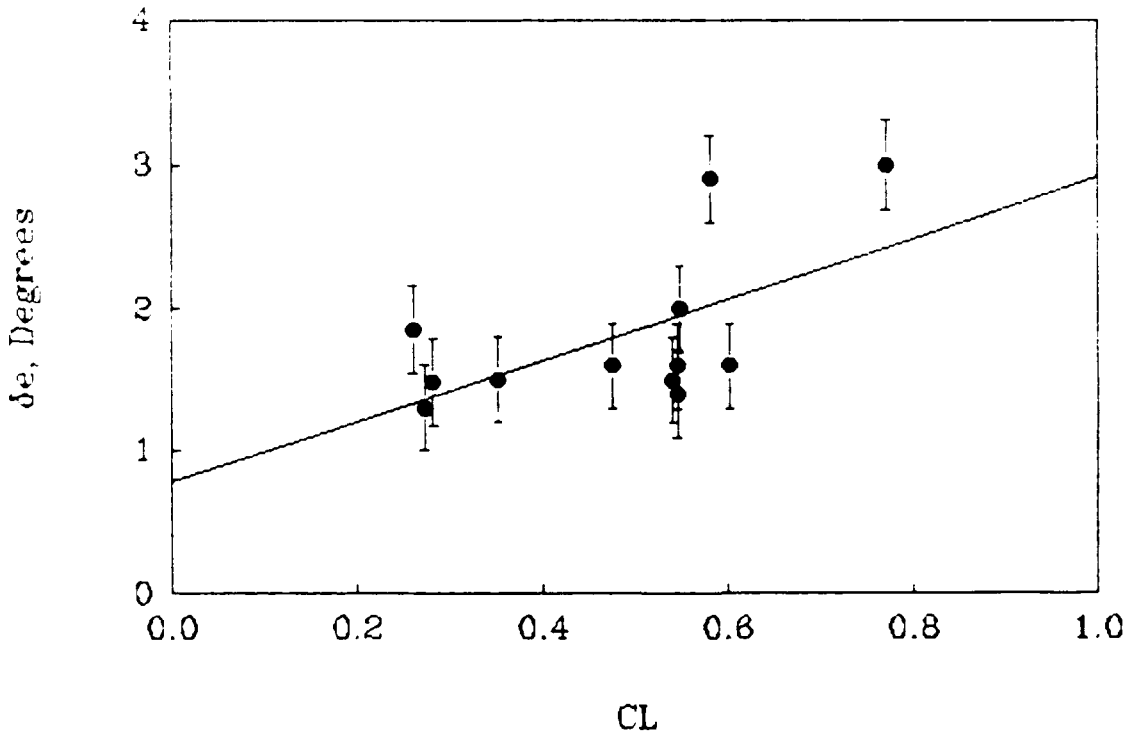

Figure 14: CG 32.9% MAC

probable error for each graph was calculated to be .32° elevator deflection for the 32.3% MAC plot and .31° elevator deflection for the 30.9% MAC plot. Probable error represents the estimate of the magnitude of the error expected in the measurements. In this case, there is a 50% chance that the actual error will fall within the probable error. [Ref. 16:p. 46]

Perusal of Figures 13 and 14 shows that as the center of gravity was moved aft, less of an elevator deflection was required to fly at an off-trim condition, or C_L. This trend would indicate that as the center-of-gravity moves aft, the aircraft becomes less stable. These results are in agreement with longitudinal static stability theory.

The slope of these curves can be plotted against the center-of-gravity positions, and fitted with a least-squares regression to produce a line whose X-axis intercept will be the aircraft's neutral point. Figure 15 is a plot of $d\delta_e/dC_L$ versus center-of-gravity position for this flight test. From this plot, the neutral point of the Pioneer was determined to be 41.2% MAC. This is in reasonable agreement with a neutral point of 47% MAC estimated by Aitcheson [Ref. 12:p. 41] using equation 4.3. This value also compares with fair agreement to the neutral point determined for the full-scale, small-tail Pioneer by Lyons [Ref. 7:p. 67] of 51% MAC. Unfortunately, no determination was made by either Aitcheson or Salmons [Ref. 11] on the Pioneer's neutral point based on flight test data.

On the last flight in this series, the Pioneer experienced a departure from controlled flight on the landing flare, partly due to the aft center-of-gravity location and partly due to the local winds at the airfield, which had become substantial. The Pioneer impacted the ground at a 90° right angle of bank, damaging the right wing and α-ß probe. Damage was major, but repairable. The wing was repaired and a new α-ß probe was manufactured.

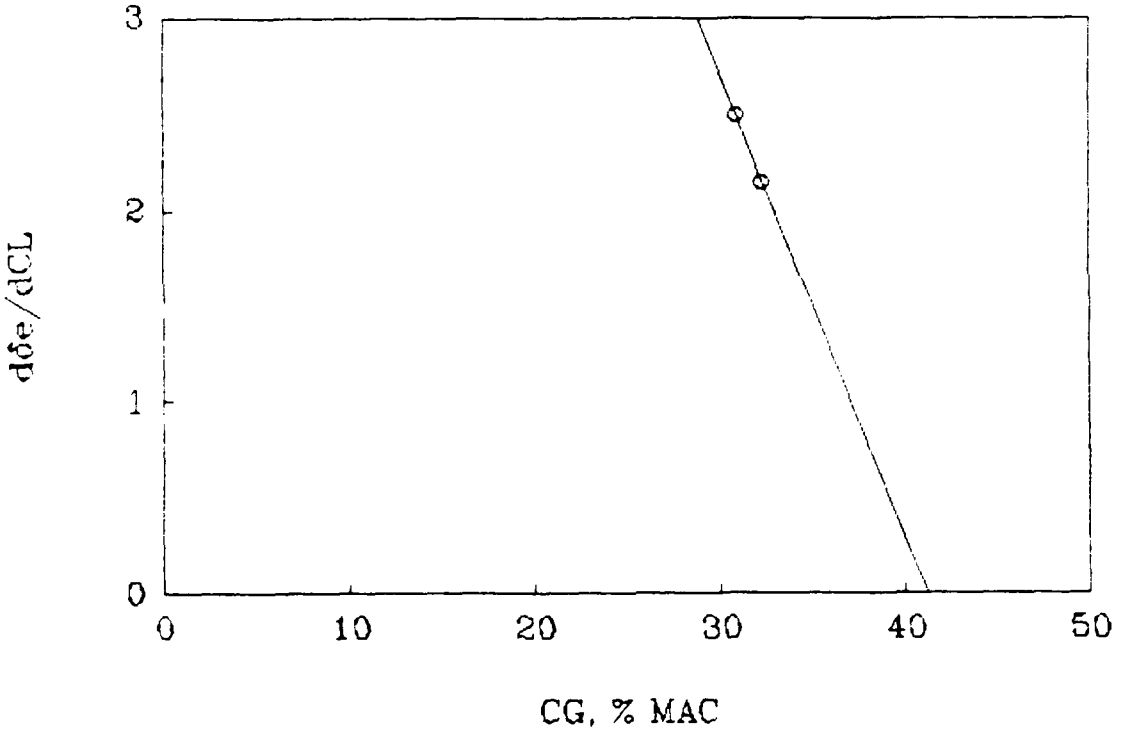

Figure 15: $d\delta_e/dC_L$ vs CG Position

B. FAMILIARIZATION FLIGHT

After the repairs were made to the Pioneer, a familiarization flight was scheduled to be flown at Fritzsche

Field. The only expectations were to ensure that the telemetry unit was operational and to provide the UAV-FRL technician pilot with refamiliarization flight-time. After 217 seconds of flight, the Pioneer experienced loss of its control signal from the flight control transmitter and impacted the ground. Damage was extensive and beyond repair.

The Pioneer was recovered, and a comprehensive check of the flight control and telemetry system components was conducted. There were no indicated problems with either system as the battery, airborne receiver and downlink were all operational. In an effort to determine the cause of the mishap, the telemetry data obtained during the flight were closely examined.

Normally, the data were sampled, then averaged to determine an output value. In this investigation, however, it was necessary to look at a time history trace of the telemetry data to visualize the control deflections and angle of attack and sideslip perturbations. It was estimated that the highest frequency signal of interest in our case was on the order of 5 Hz. Nyquist sampling theory would suggest a sampling rate of twice this to prevent aliasing, in our case 10 Hz. However, a sampling rate of 100 Hz was chosen to compensate for unavoidable distortion caused by the filtering process. The investigation called for the analysis of the entire flight, which study uncovered some interesting discoveries.

Figure 16 shows the telemetry data from early in the familiarization flight. The angle-of-attack data were unusable due to previous problems with the α-ß probe. The remainder of the channels were operational, and no unusual indications were present. Figure 17 shows a ten-second time trace 175-185 seconds into the same flight. Between approximately five and seven seconds into the trace there were some unusual indications. The telemetry data, for example, indicated a rudder deflection rate of 48°/sec, while sideslip angle remained constant for a full second. While the rudder deflection is within the limits of the servos, the indicated result offers little explanation to the aerodynamic behavior of the Pioneer. Figure 18 shows a similar incident, approximately 215 seconds into the flight. As in the last trace, there were some inconsistencies. For example, a 50° change in sideslip angle was indicated with no corresponding rudder input. Also, the airspeed channel indicated a 20 KIAS change in airspeed in 0.25 seconds. The flight ended with the Pioneer impacting the ground at approximately 217 seconds. Again, the telemetry data indicated rapid and extreme control surface deflections in the seconds prior to impact. When the telemetry data were viewed concurrently with a video tape of the flight, the behavior of the Pioneer was not consistent with the telemetry indications. Rather, both incidents were

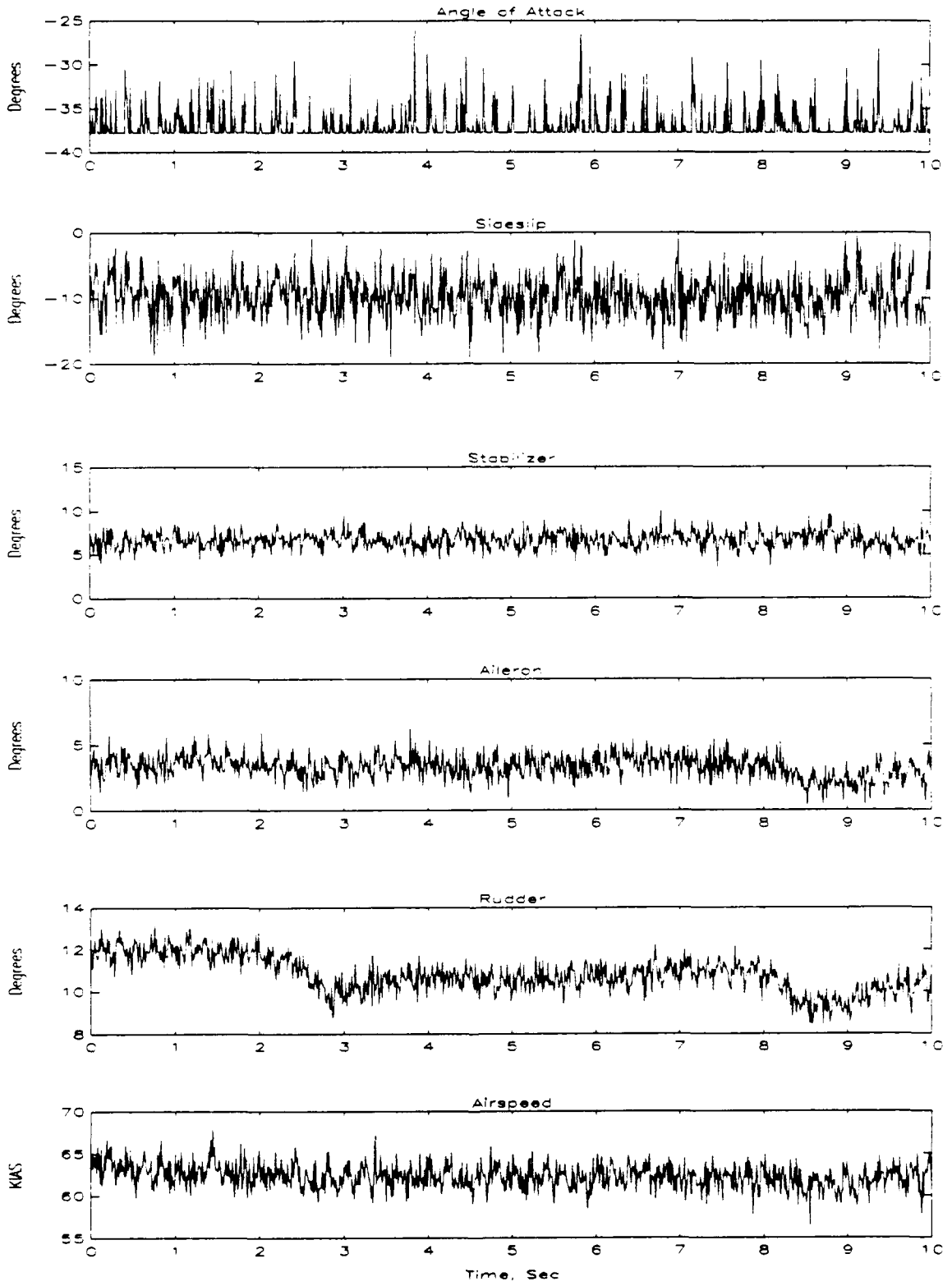

Figure 16: Normal Flight

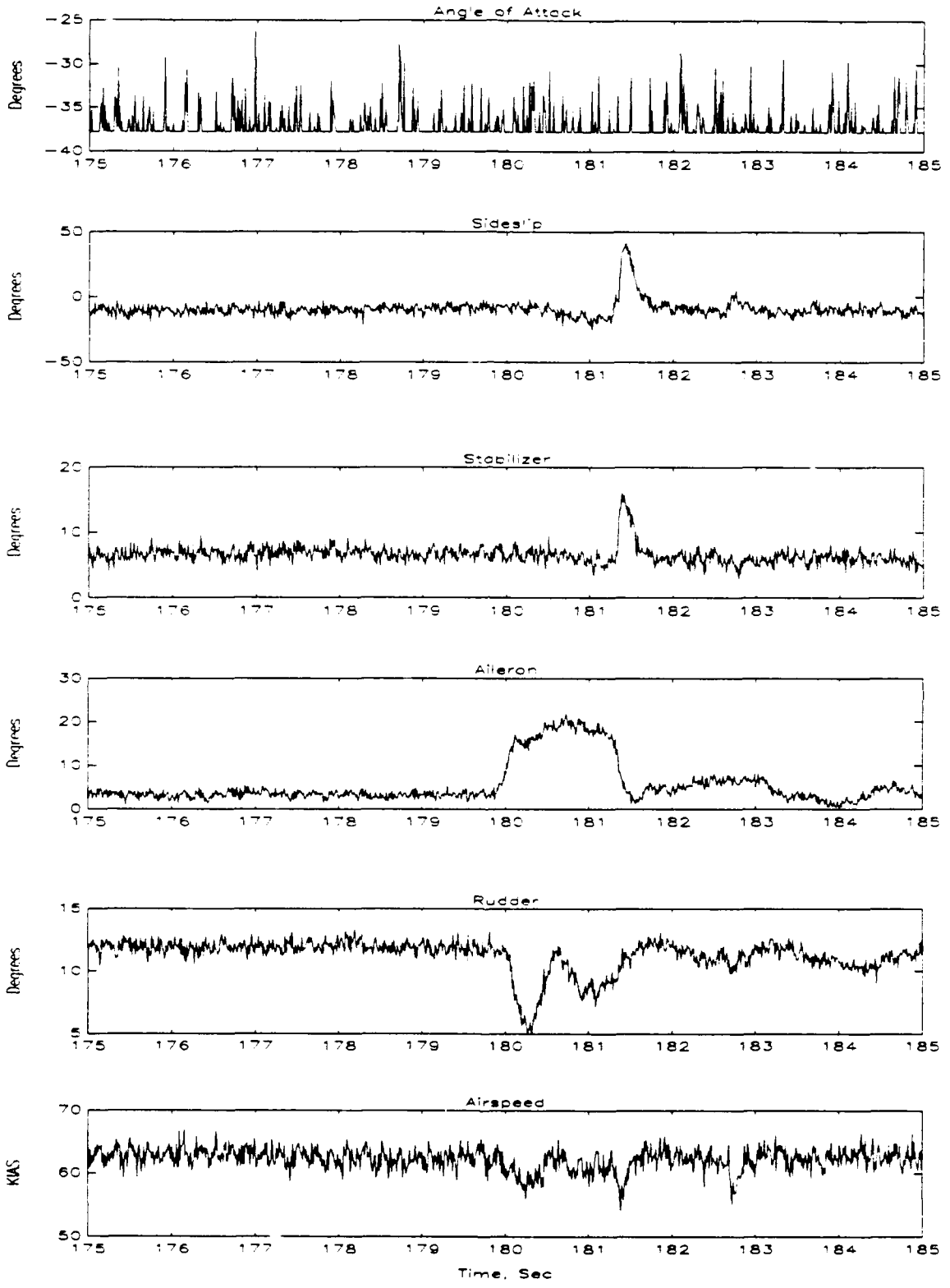

Figure 17: 175-185 Seconds

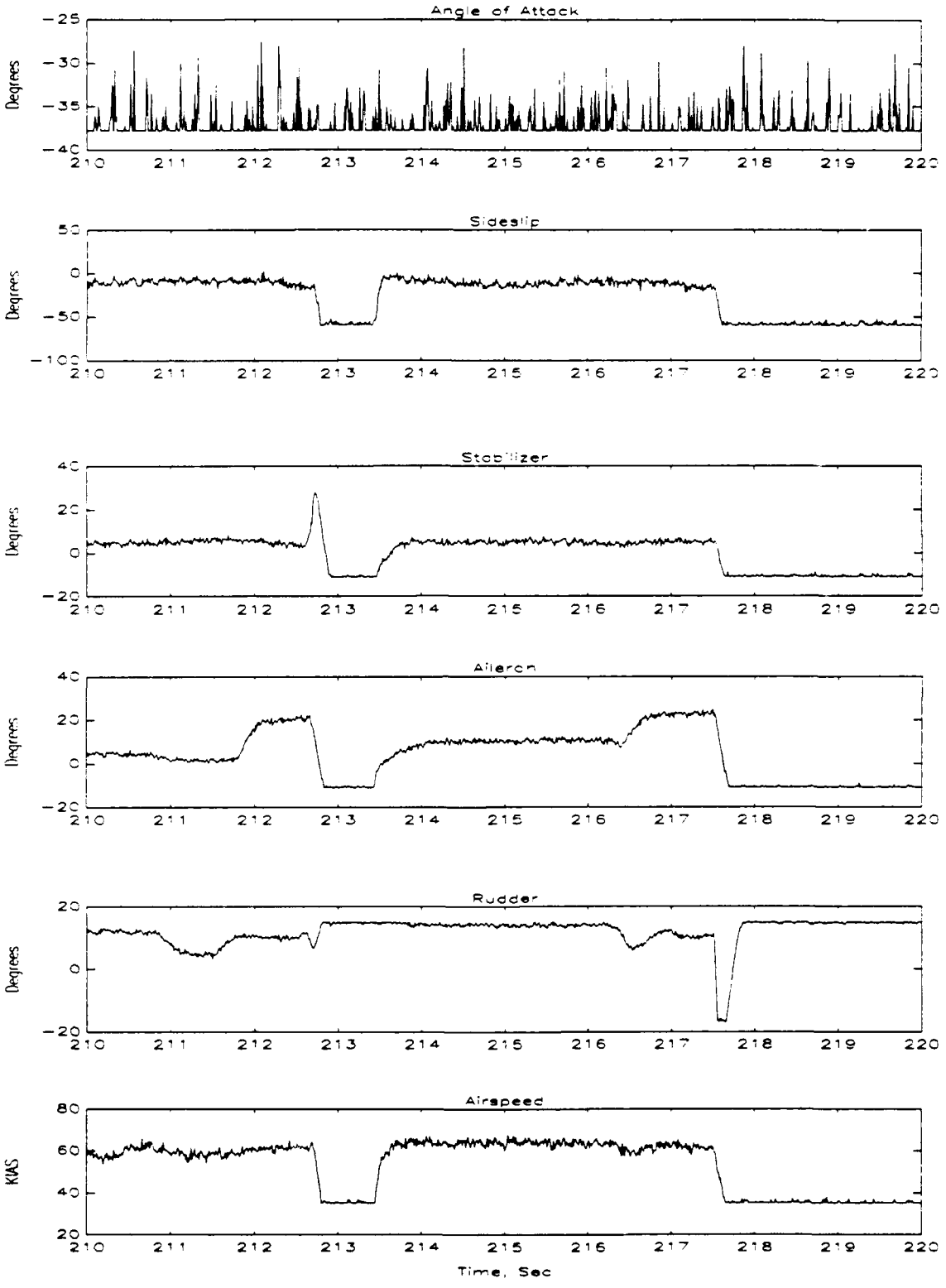

Figure 18: 210-220 Seconds

indicative of loss of the control signal from the receiver. In the first incident, the Pioneer regained the signal. In the second incident, the control signal was lost until impact.

There could be several explanations for the interruption of the control signals to the Pioneer. Among the most likely is the corruption of the signal by some type of electromagnetic interference (EMI). Electromagnetic noise from power lines, radio and television broadcasts, cellular phones, and citizen band and ham radio transmissions are all examples of signals that could corrupt the flight control signal to the Pioneer. The most likely source of EMI, in our case, is that from the operations of the military helicopters that were within several thousand feet of the test area. Previous flights flown at Fritzsche Field were flown on weekend days, when there was no helicopter activity. This last flight, however, was flown on a weekday, when there was heavy helicopter activity. Radar, UHF radio transmissions, and other relatively high-powered transmitters could easily disrupt the weak 500 mW signal from the flight control transmitter, in addition to corrupting the 600 mW downlink signal from the telemetry transmitter.

C. DATA FILTERING

Although the data in Figures 16-18 are apparently scattered about a mean value, it was decided to filter all the channels using a Butterworth digital filtering routine from

the MATLAB signal processing utility library to remove as much noise as possible from the data.

Before filtering, a power spectral density plot was compiled for the data to show the various frequency components. Figure 19 shows that some signals were present above 5 Hz, but the majority of the signals, the signals of particular interest, were located 5 Hz and below.

A second-order Butterworth filter was constructed to filter all signals above 5 Hz. A Butterworth filter is essentially a low-pass digital filter design with a selectable cut-off frequency, with all signals above the cut-off frequency filtered out. In our case, a cut-off frequency of 5 Hz was chosen.

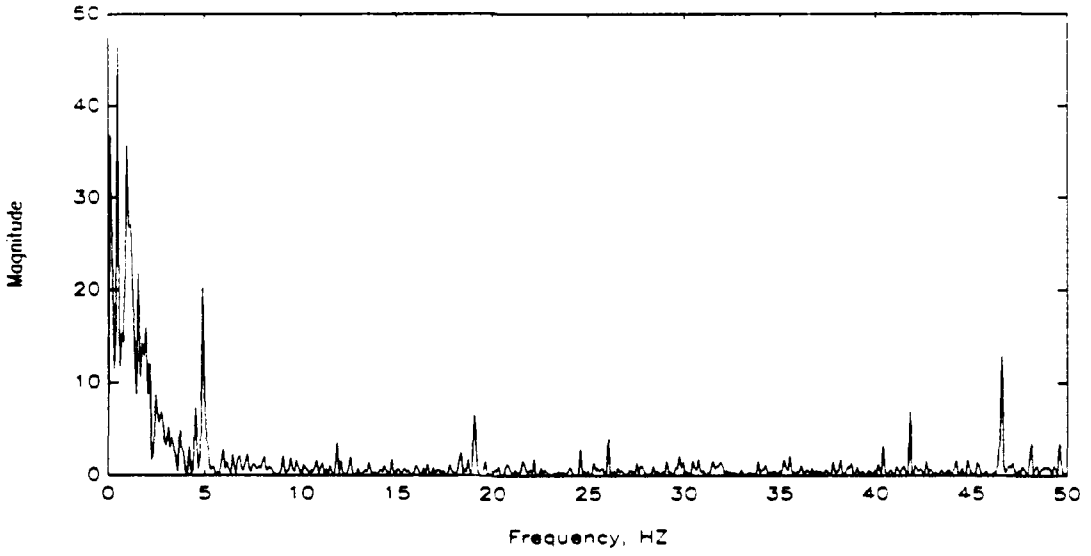

Figure 19: Power Spectral Density

As mentioned earlier, a sampling rate of 10 times the Nyquist recommended sampling rate was chosen. This choice was to help compensate for the distortion introduced by filtering the data. The sampling theorem states that if a signal is band-limited and contains only frequencies below the cut-off frequency, then the continuous signal is completely recoverable, if sampled at a rate above the Nyquist frequency. When the data are filtered, however, recovery is not complete, due to in part to the inadequacy of the digital filter design. [Ref. 17:p. 28]

Figures 20-22 show the filtered data of the previous Figures 16-18. By filtering the data, it is clearly much easier to identify the control surface deflections and aircraft parameter fluctuations.

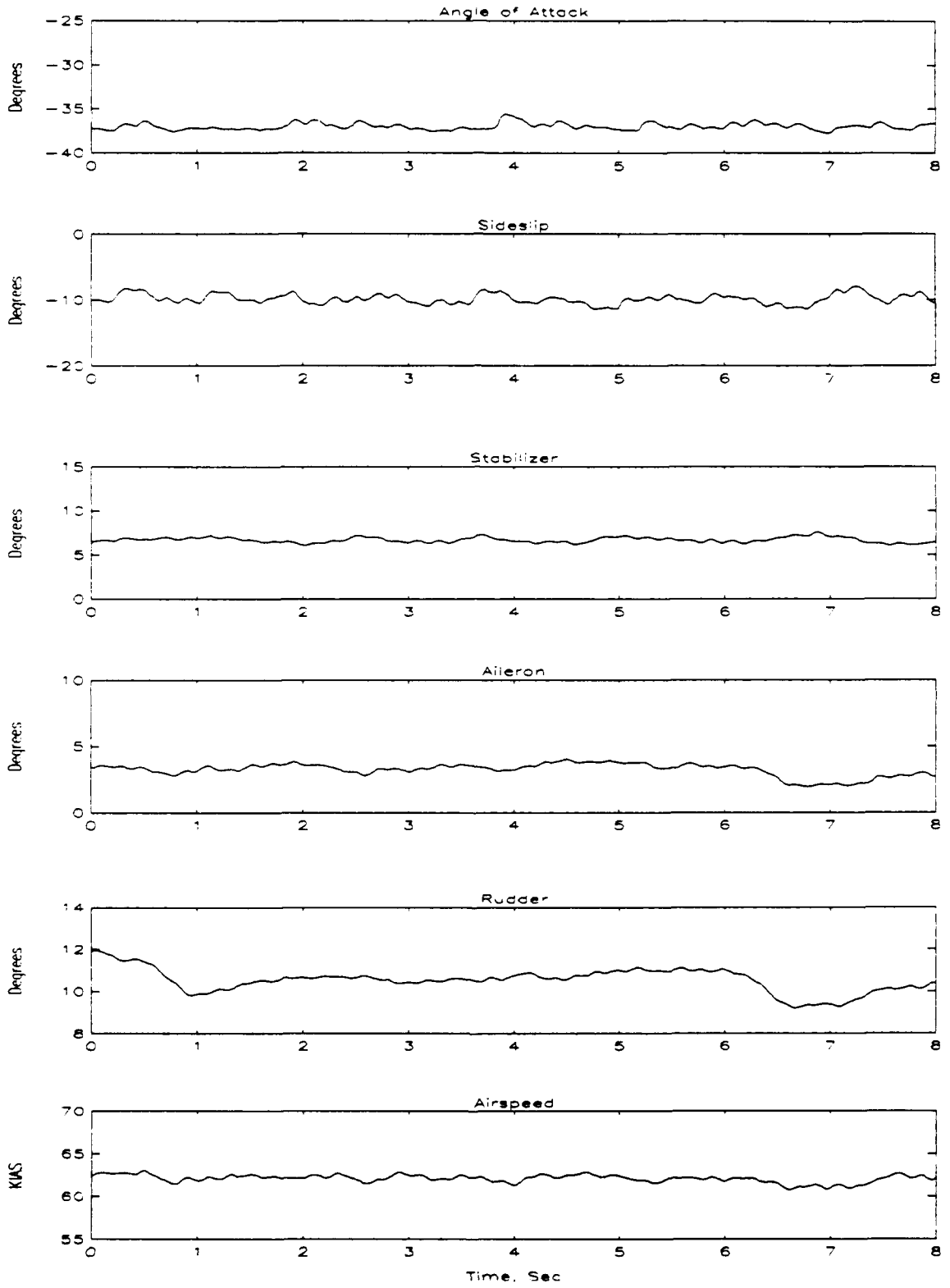

Figure 20: Normal Flight (Filtered Data)

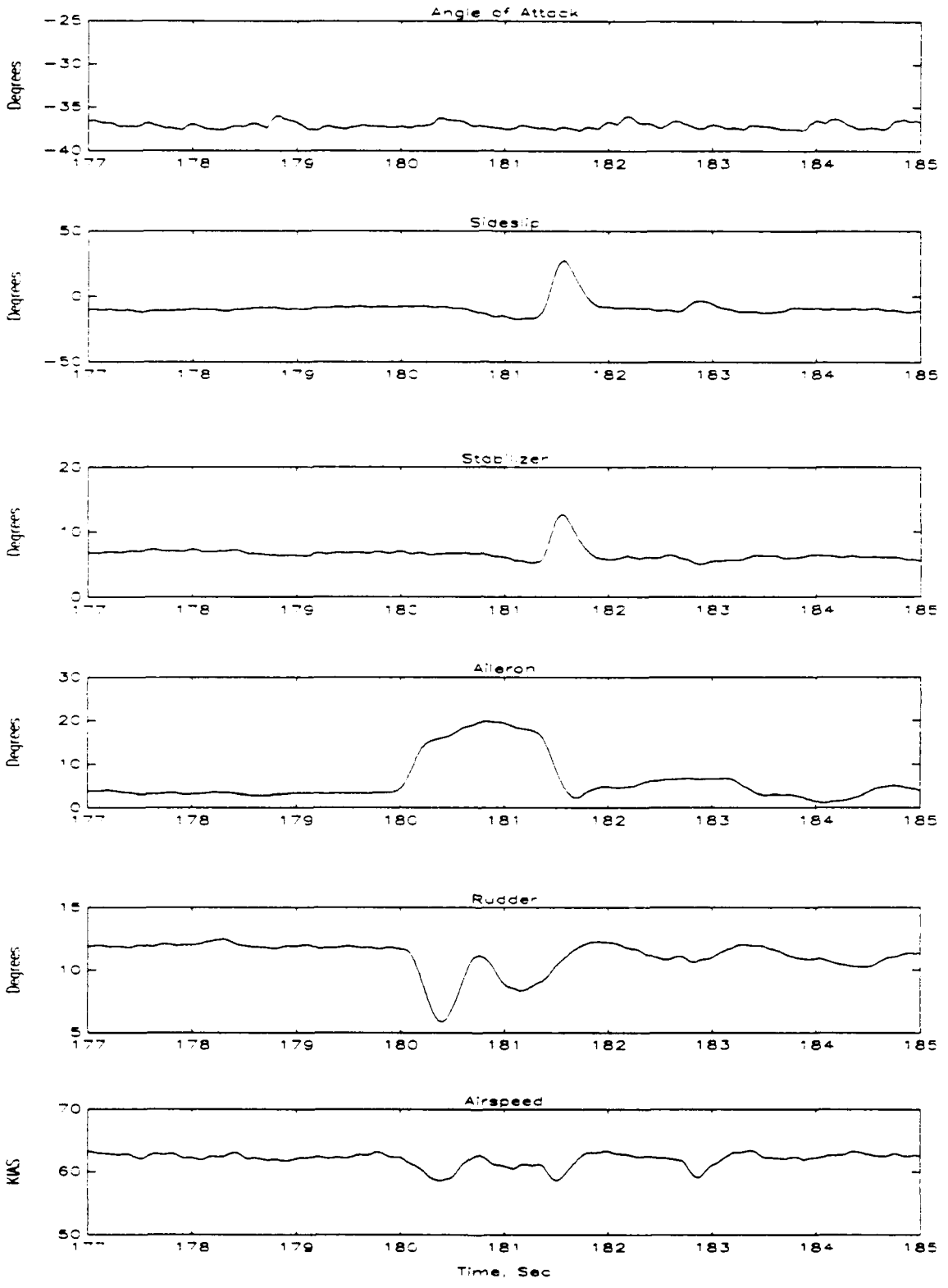

Figure 21: 177-185 Seconds (Filtered Data)

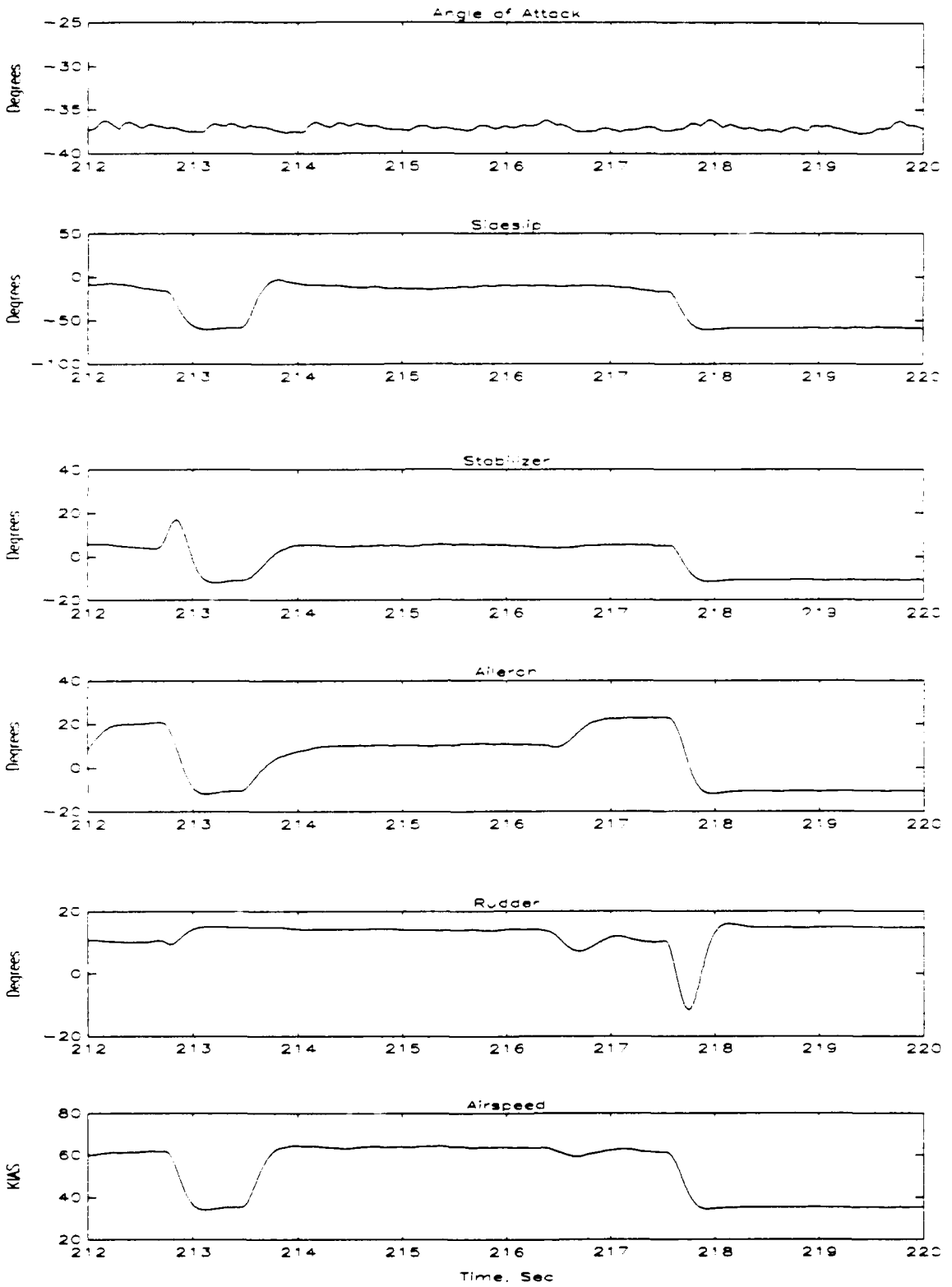

Figure 22: 212-220 Seconds (Filtered Data)

VI. CONCLUSIONS AND RECOMMENDATIONS

A. CONCLUSIONS

The telemetry system worked well during both the longitudinal static stability flight testing and the familiarization flight. There were problems with the angle-of-attack data due to undetermined problems with the α-ß probe, but all other channels functioned properly.

The results of the longitudinal static stability flight testing correlated well with theoretical predictions [Ref. 12] and with data obtained from full-scale Pioneer computer simulation [Ref. 7]. Use of the Labtech Notebook and MATLAB software made time-history analysis of flight test data possible for possible future implementation into parameter estimation routines to determine aircraft stability and control derivatives.

The last flight of the Pioneer showed in dramatic fashion the problems of EMI. Although unfortunate, some valuable lessons were learned that will prevent such incidents in the future.

B. RECOMMENDATIONS

Before commencing further UAV flight testing, the problem of EMI must be investigated. The best way to control the effects of EMI is to avoid it. While complete isolation from the effects of EMI is difficult, a flight test area free from

the effects of EMI is difficult, a flight test area free from known EMI source should be established in the future to prevent a similar incident.

As mentioned earlier, the Pioneer flights were recorded on videotape. Closer synchronization between telemetry tapes and the video tapes will help in later analysis of flights.

The data acquisition system can be expanded to include such parameters as roll rate, yaw rate, pitch rate and normal acceleration, with minor changes to the existing CHOW-1G telemetry unit. An upgraded IBM 386-type personal computer with a larger memory capacity would allow for higher sampling rates, reducing sampling errors and allowing for the storage of the telemetry data for an entire flight. Additionally, a portable laptop computer would enhance the data acquisition and reduction process by allowing for real-time data acquisition and immediate post-flight parameter estimation at the test site.

APPENDIX A: CALIBRATION

Calibration began by energizing the CHOW-1G telemetry unit, the flight control receiver unit and the flight control transmitter unit. With these units powered, the control servos were also powered to their neutral position. A 15-pin test connector (Fig. 23) was attached to the telemetry unit test plug which was in turn connected to the circuit board (Fig. 24). The telemetry unit voltage output for each channel was measured using a digital voltmeter that was connected to the circuit board. Additionally, an oscilloscope was used to sample the telemetry output signal (Fig. 25).

With the control servo in their neutral positions, each control surface was visually set to neutral using the calibration gear designed by Aitcheson (Ref. 12). Figures 26-28 show the calibration set-up of the elevator, rudder and aileron.

Next, the center voltages of each potentiometer was set, including the α-ß probe. This centering was done by loosening the potentiometer set-screws, then adjusting the potentiometer position to correspond to 2.5 Vdc values when the control surfaces and angle of attack and sideslip angle were neutral. Figure 29 shows the α-ß probe calibration.

With the center voltages set, the next step was to adjust the pulsewidth of each channel to an optimum pulsewidth of 1.0

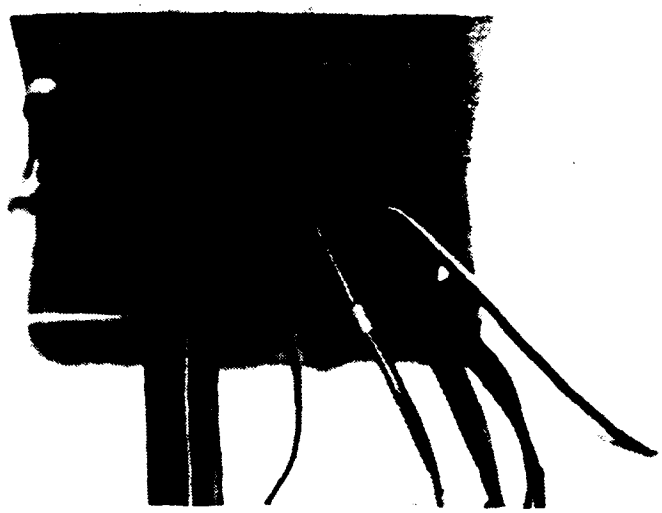

Figure 23: 15-Pin Test Connector

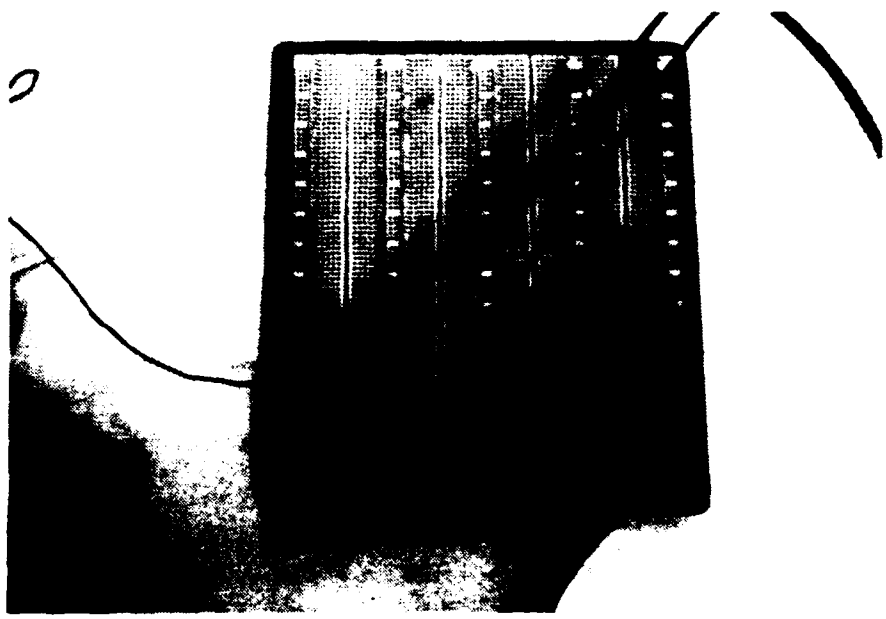

Figure 24: Circuit Board

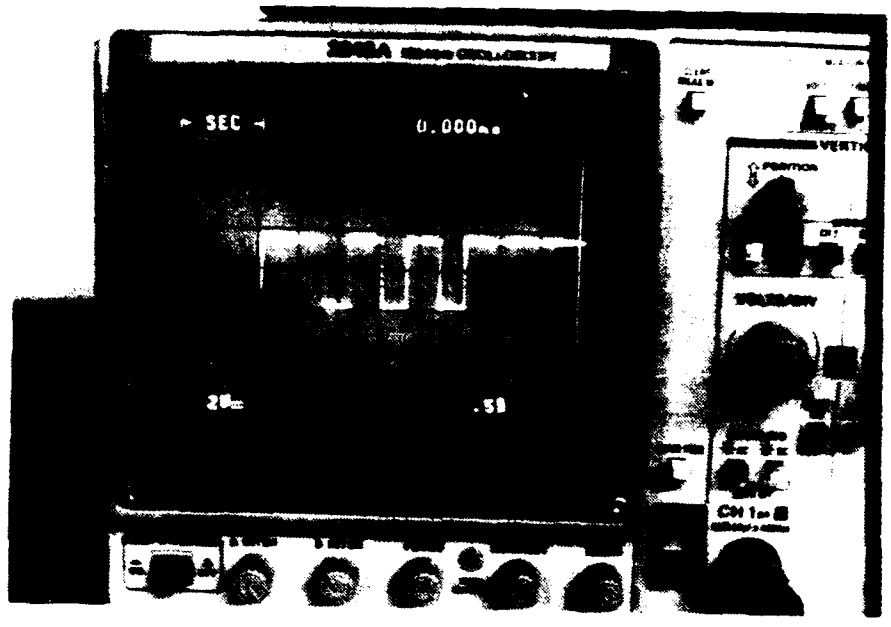

Figure 25: Oscilloscope

Figure 26: Elevator Calibration

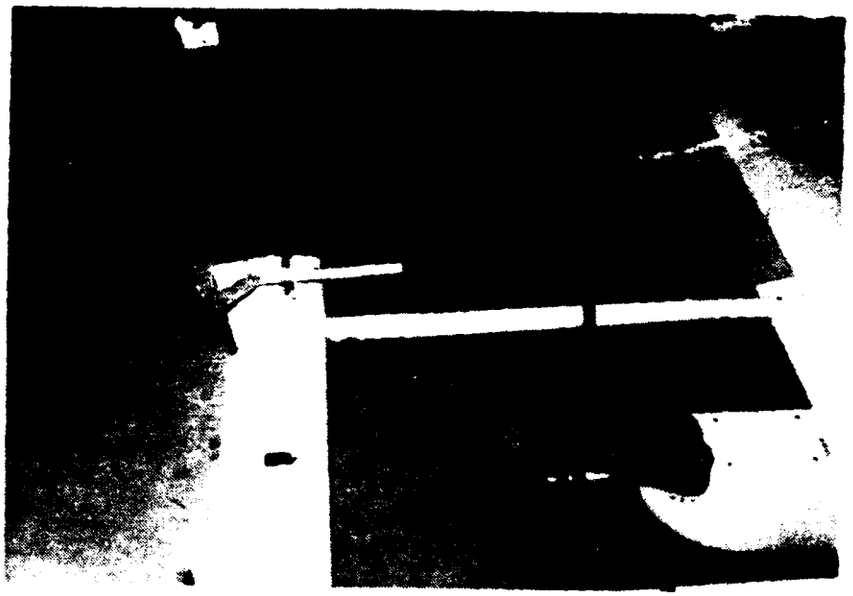

Figure 27: Rudder Calibration

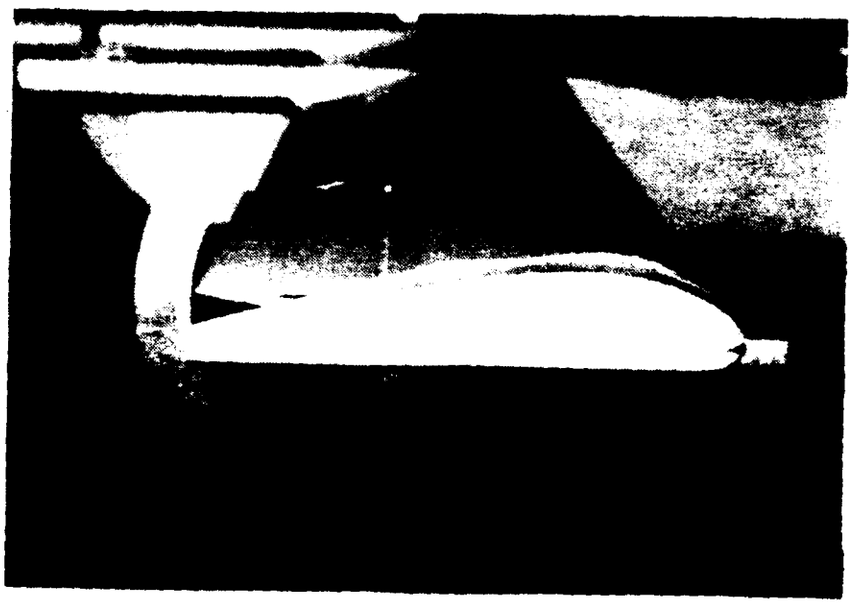

Figure 28: Aileron Calibration

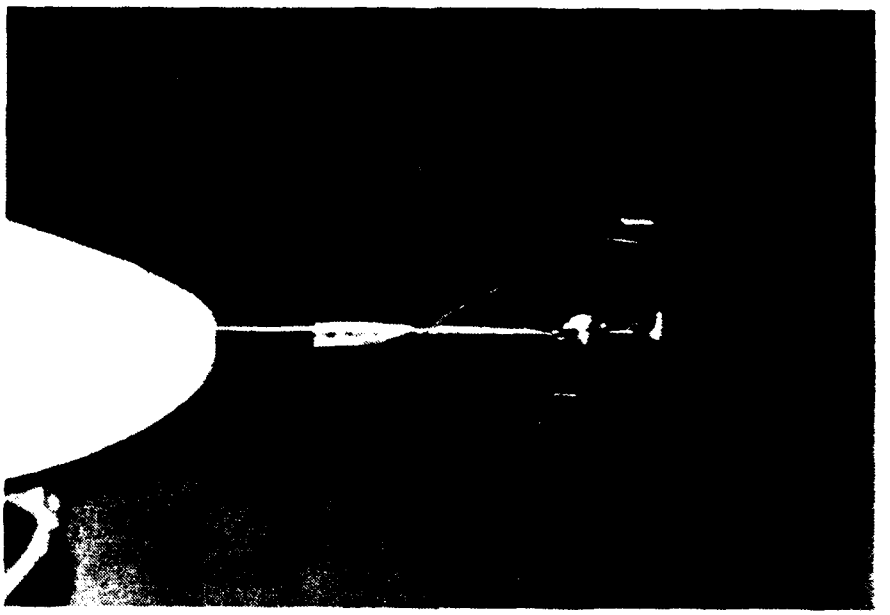

Figure 29: α-β Probe Calibration

ms. This pulsewidth calibration was done by adjusting the turn-screws on the top of the CHOW-1G, on the multiplexer circuitry. The pulsewidth was observed visually on the oscilloscope screen and adjusted accordingly. For the airspeed indicator system, the lower airspeed limit was set using the "Schmidter" pressure calibration device (Fig. 30). With the lower airspeed limit set, the lower pulsewidth was set to .5 ms. The upper limit was not adjustable, but rather was dependant on the choice of lower limit, and limited by the 1.0 ms change in pulsewidth. For this testing, a lower limit of 40 KIAS was chosen, which corresponded to an upper airspeed

limit of 8[illegible] KIAS, which occurred at a pulsewidth of 1.5 ms. This range was found to be adequate for our testing.

With the flight control and telemetry systems calibrated, the calibration file used by the REDUCE program could be

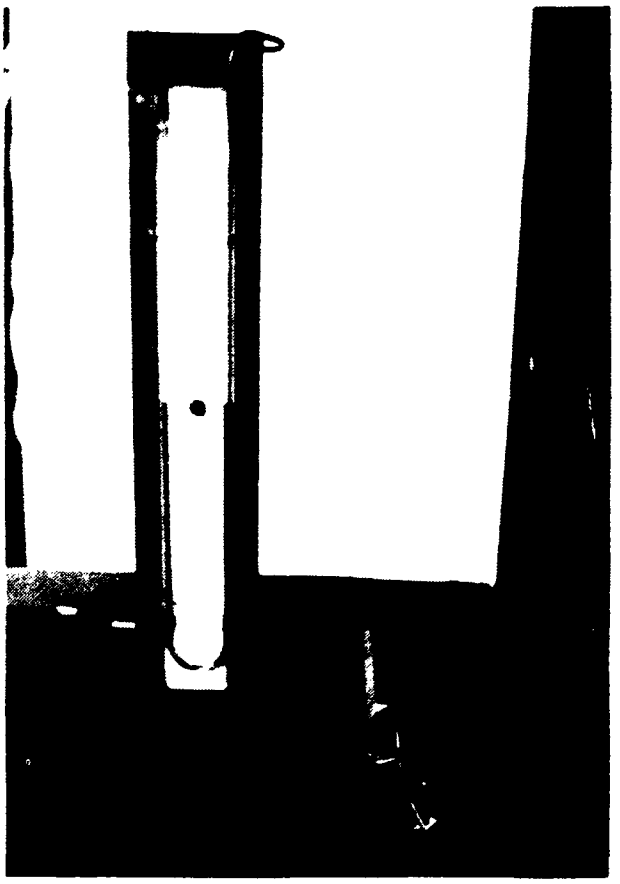

Figure 30: Schmidter Calibration Device

constructed. Three calibration points were picked (see Chapter IV) and set using the calibration tools used previously. For each point, the control surface positions, angle of attack and sideslip angle, and airspeed were set, and the data were recorded as analog voltages on magnetic tape. These data were then reduced using the REDUCE program to create an output file which was used to calibrate flight data collected later.

APPENDIX B: LONGITUDINAL STATIC STABILITY DATA

TABLE 1: FLIGHT ONE

α	ß	δ_e	δ_a	δ_r	V	C_L
-37.81	56.71	1.84	-2.69	6.82	68.45	.260
-37.34	56.43	1.55	-2.17	4.86	50.64	.475
-37.27	56.22	1.58	-1.74	2.19	47.26	.545
-37.27	56.32	1.96	-2.79	6.39	47.16	.548
-37.32	56.31	3.07	-2.10	2.77	39.74	.771
-38.17	57.02	1.29	-2.46	5.53	66.84	.273
-38.16	57.03	1.45	-2.90	1.34	47.29	.545
-37.86	56.69	1.67	-2.59	3.98	44.96	.602
-37.66	56.68	2.92	-1.44	5.99	45.76	.582
-37.59	56.55	1.47	-1.67	5.20	65.80	.281
-36.93	56.03	1.49	-1.99	-2.95	58.85	.352
-37.16	56.28	1.49	-2.00	1.30	47.47	.540

TABLE 2: FLIGHT TWO

α	ß	δ_e	δ_a	δ_r	V	C_L
-36.73	55.52	4.42	-2.26	6.02	55.68	.275
-36.82	55.82	2.18	-1.74	5.62	67.15	.275
-36.56	55.63	2.16	-1.97	1.00	53.07	.440
-36.84	55.81	1.59	-1.49	-.87	52.59	.448
-36.47	55.55	2.40	-2.50	-1.95	51.92	.460
-36.59	55.67	1.89	-1.69	.83	49.06	.515
-36.76	55.78	2.47	-.79	-2.90	42.18	.696
-36.84	55.83	2.73	.33	-1.11	38.32	.844
-36.68	55.71	3.16	-2.30	5.14	39.37	.799
-36.22	55.36	3.26	-1.28	3.48	38.46	.840
-36.47	55.55	4.16	-2.66	2.27	36.50	.930
-36.45	55.53	2.14	-1.89	3.38	67.50	.272

LIST OF REFERENCES

1. American Institute of Aeronautics and Astronautics Paper 88-2146, *Radio Controlled Model Flight Tests of a Spin Resistant Trainer Configuration*, Yip, Long P., Robelen, David B., and Meyer, Holly F., 1988.

2. American Institute of Aeronautics and Astronautics Paper 90-1261, *Wind Tunnel and Flight-Test Investigation of the Exdrone Remotely Piloted Vehicle Configuration*, Yip, Long P., Robelen, David B, and Makowiec, George M., 1990.

3. NASA Technical Publication 4108, *Lateral Stability Analysis for X-29A Drop Model using System Identification Methodology*, by Raney, David L., and Batterson, James G., June 1989.

4. Howard, Richard M., Lyons, Daniel F., and Tanner, James C., "Research Flight Testing of a Scaled Unmanned Air Vehicle," Society of Flight Test Engineers 12th Annual Symposium Proceedings, 1990.

5. Shaker, Steven M., Wize, Alan R., *War Without Men: Robots on the Future Battlefield*, Pergamon-Brassey's International Defense Publishers, 1988.

6. Rumpf, Richard and Barr, Irwin, "Pioneer is Operationally Capable," *Aerospace America*, February 1989.

7. Lyons, Daniel F., *Aerodynamic Analysis of a U.S. Navy and Marine Corps Unmanned Air Vehicle*, Master's Thesis, Naval Postgraduate School, Monterey, California, June 1989.

8. Philpott, Tom, "Unmanned 'Toy' Played Big Role in U.S. Targeting of Iraqi Forces," *Navy Times*, March 11, 1991.

9. "Gulf War Experience Sparks Review of RPV Priorities,"*Aviation Week & Space Technology*, April 22, 1991.

10. Tanner, James C., *Development of a Flight Test Methodology for a U.S. Navy Half-Scale Unmanned Air Vehicle*, Master's Thesis, Naval Postgraduate School, Monterey, California, March 1989.

11. Salmons, James D., *Developmental Flight Testing of a Half-Scale Unmanned Air Vehicle*, Master's Thesis, Naval Postgraduate School, Monterey, California, September 1990.

12. Aitcheson, Kent R., *Stability and Control Flight Testing of a Half Scale PIONEER Remotely Piloted Vehicle*, Master's Thesis, Naval Postgraduate School, Monterey, California, September 1991

13. Wilhelm, Kevin T., *Development and Testing of an Unmanned Air Vehicle Telemetry System*, Master's Thesis, Naval Postgraduate School, Monterey, California, September, 1991.

14. Roberts, Sean C., "Flying Qualities Flight Testing of Light Aircraft for Test Pilots and Engineers," Flight Research Inc., 1982.

15. Anderson, John D., *Introduction to Flight*, McGraw-Hill, 1989.

16. Bevington, Philip, R., *Data Reduction and Error Analysis for the Physical Sciences*, McGraw-Hill, 1969.

17. Beauchamp, K., Yuen, C., *Digital Methods for Signal Analysis*, George, Allen & Unwin, 1979.

INITIAL DISTRIBUTION LIST

	No. Copies
1. Defense Technical Information Center Cameron Station Alexandria, Virginia 22304-6145	2
2. Library, Code 52 Naval Postgraduate School Monterey, California 93943-5002	2
3. Chairman, Code AA Department of Aeronautics and Astronautics Naval Postgraduate School Monterey, California, 93943-5000	1
4. Professor Richard M. Howard, Code AAHo Department of Aeronautics and Astronautics Naval Postgraduate School Monterey, California 93943-5100	3
5. LT Paul A. Koch 3689 350th Avenue West Oak Harbor, Washington 98277	3
6. Mr. Richard J. Foch Naval Research Laboratory Code 5712 4555 Overlook Avenue S.W. Washington, D.C. 20374	1
7. Mr David Lewis Unmanned Aerial Vehicles Joint Project PEO (CU)-UD Washington, D.C. 20361-1014	1
8. Short-Range Program Unmanned Aerial Vehicles Joint Project PMA 263 Washington, D.C. 20361-1263	1
9. Keith Bratburg Target Simulation Lab PMTC Code 1074 Pt Mugu, California 93042-5000	1